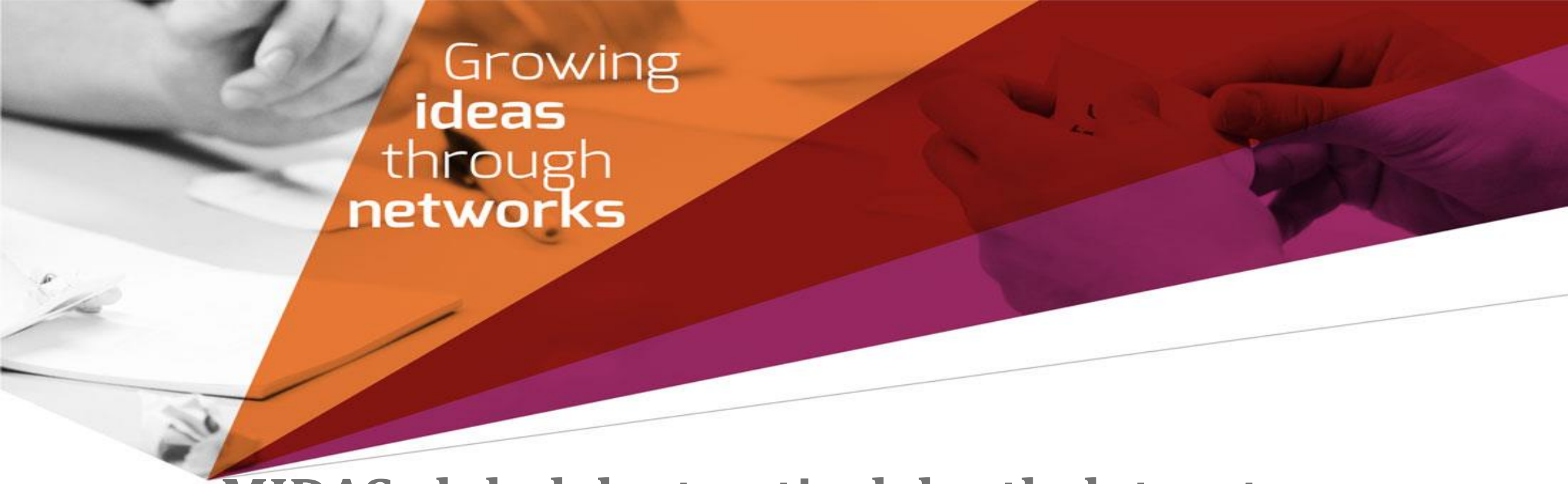



# MIDAS global dust optical depth dataset: Development and applications

**Antonis Gkikas**

National Observatory of Athens (NOA)

cost
EUROPEAN COOPERATION
IN SCIENCE & TECHNOLOGY

Funded by the Horizon 2020 Framework Programme
of the European Union

# Outline

**MIDAS development**

**Climatology and trends**

**Radiative effects**

**Data assimilation**

**Dust sources identification**

cost
EUROPEAN COOPERATION IN SCIENCE & TECHNOLOGY

# MIDAS development

cost
EUROPEAN COOPERATION
IN SCIENCE & TECHNOLOGY

# ModIs Dust AeroSol (MIDAS)

Atmos. Meas. Tech., 14, 309–334, 2021
https://doi.org/10.5194/amt-14-309-2021
© Author(s) 2021. This work is distributed under
the Creative Commons Attribution 4.0 License.

Atmospheric Measurement Techniques
Open Access
EGU

## ModIs Dust AeroSol (MIDAS): a global fine-resolution dust optical depth data set

Antonis Gkikas[1], Emmanouil Proestakis[1], Vassilis Amiridis[1], Stelios Kazadzis[2,3], Enza Di Tomaso[4], Alexandra Tsekeri[1], Eleni Marinou[5], Nikos Hatzianastassiou[6], and Carlos Pérez García-Pando[4,7]

## Features of the **ModIs Dust AeroSol (MIDAS)** dataset:

- **Columnar dust optical depth (DOD) at 550 nm**
- **Spatial/Temporal resolution:** 0.1° x 0.1° / Daily
- **Spatial coverage:** Global (both over land and ocean)
- **Temporal availability:** 2003 – 2017 (15 years)
- **Data access:** https://zenodo.org/record/4244106#.YGyN4S0RrOQ

# Current status and added value

- Fine spatial resolution (Ginoux et al., 2012) **but restricted over land**
- Global coverage (e.g., Ridley et al., 2016; Voss and Evan, 2020; Song et al., 2021) **but at coarse spatial resolution**
- Based on active remote sensing retrievals (Amiridis et al., 2015) **which are strongly dependent by the assumption of the lidar ratio**
- Aerosol retrievals at thermal infrared (TIR) wavelengths (e.g., Vandenbussche et al., 2013) **in which the conversion of DOD from TIR to the mid-VIS is subjected to several assumptions (e.g., size properties)**
- Model-derived (e.g., Gliß et al., 2021) and reanalysis datasets (e.g., Gelaro et al., 2017) **driven by assumptions in the dust parametrization schemes and they are available at coarse spatial resolution**

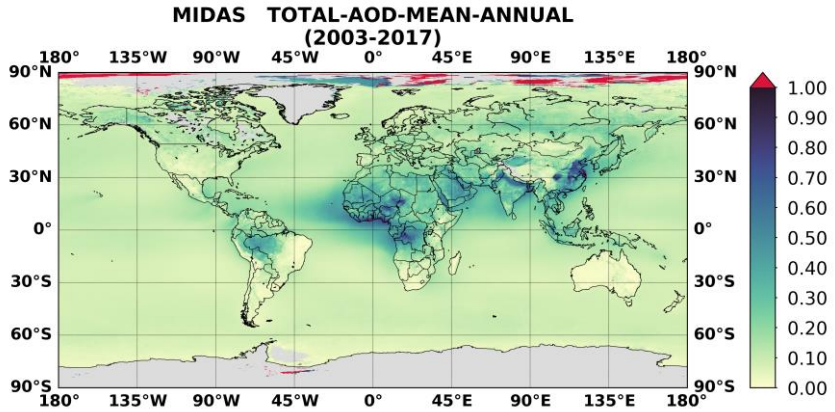
Based on the current status, **MIDAS expands**, **complements**, and **upgrades** existing **observational capabilities of dust aerosols**, being suitable for research studies related to **climatology**, **model evaluation**, and **data assimilation**.

cost
EUROPEAN COOPERATION IN SCIENCE & TECHNOLOGY

# Overview of the applied methodology

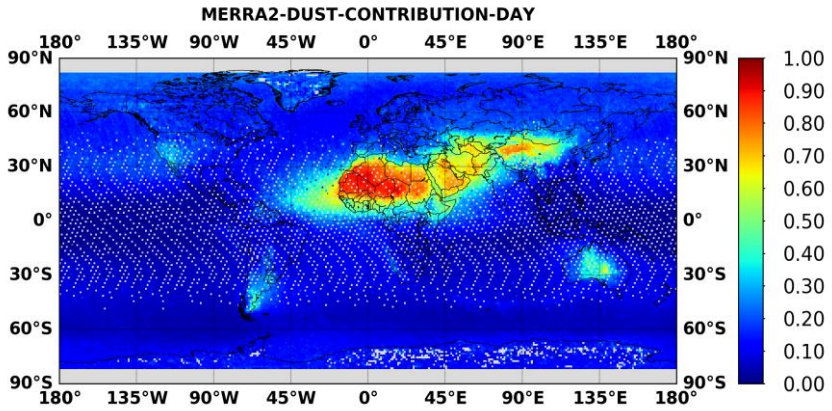
**MODIS-Aqua $AOD_{550nm}$**

**Derivation of MIDAS DOD [MODIS-MERRA-2]**

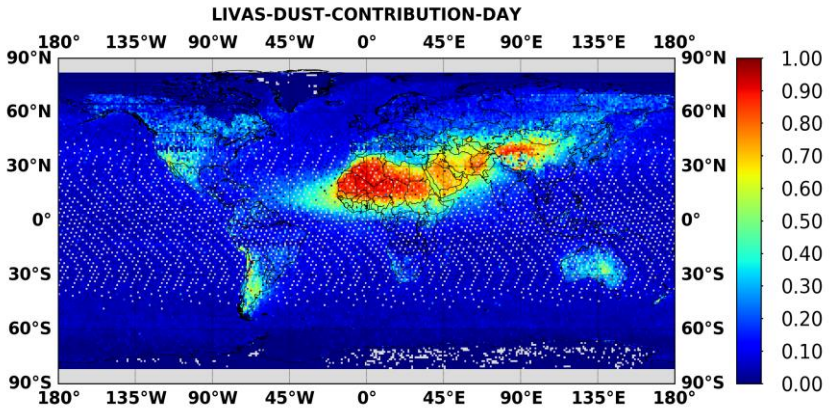


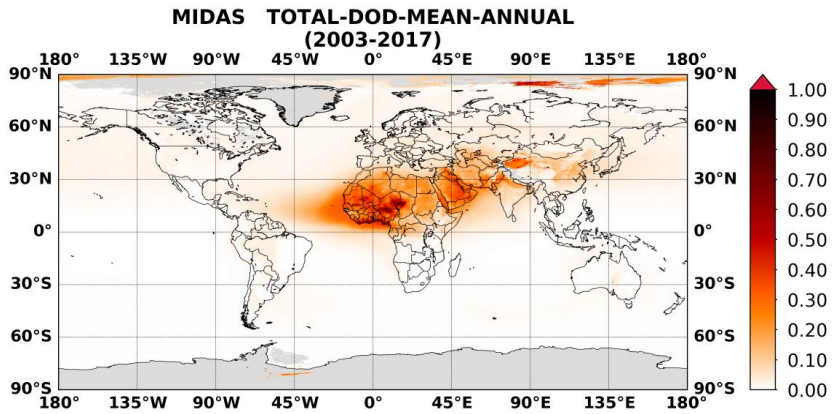

**Evaluation of MDF vs LDF**

**MERRA-2 Dust Fraction (MDF)**




**LIVAS Dust Fraction (LDF)**




- **Evaluation vs AERONET**
- **Intercomparison against MERRA-2 and LIVAS**

**MIDAS $DOD_{550nm}$**

# Derivation of MIDAS DOD

| MERRA-2 |
| --- |
| **Database:** Modern-Era Retrospective analysis for Research and Applications, Version 2 (MERRA-2) [Randles et al., 2017] |
| **SDS:** Total and dust extinction at 550 nm |
| **Spatial/Temporal resolution:** 0.5° x 0.625° (lat-lon) / hourly |

| MODIS - Aqua |
| --- |
| **Sensor:** MODerate resolution Imaging Spectroradiometer [Levy et al., 2013] |
| **SDS:** AOD at 550 nm (Collection 6.1) ➔ **quality screened** |
| **Spatial/Temporal resolution:** 10km x 10km (nadir) / 5min (Level 2) |

$$MDF = \frac{AOD_{DUST;MERRA-2}}{AOD_{TOTAL;MERRA-2}}$$

Contribution of DOD to the total AOD based on MERRA-2 reanalysis

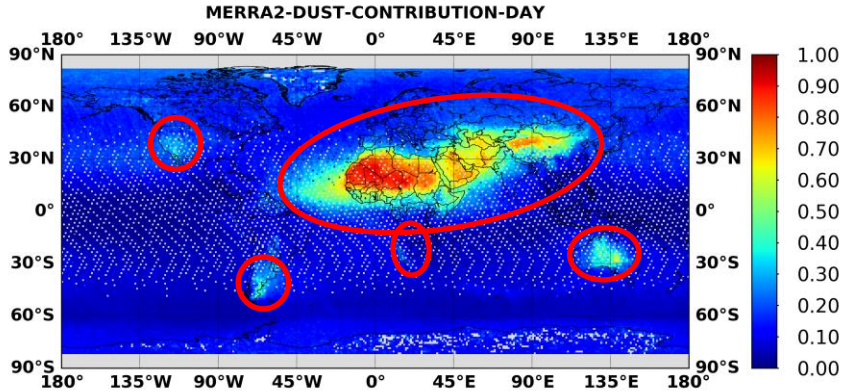
$$DOD_{MIDAS} = AOD_{MODIS} * MDF$$

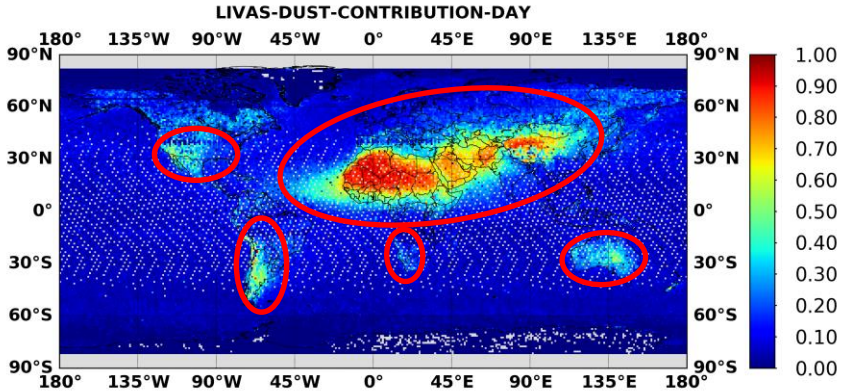
Derivation of MIDAS DOD from MODIS AOD Level 2 retrievals

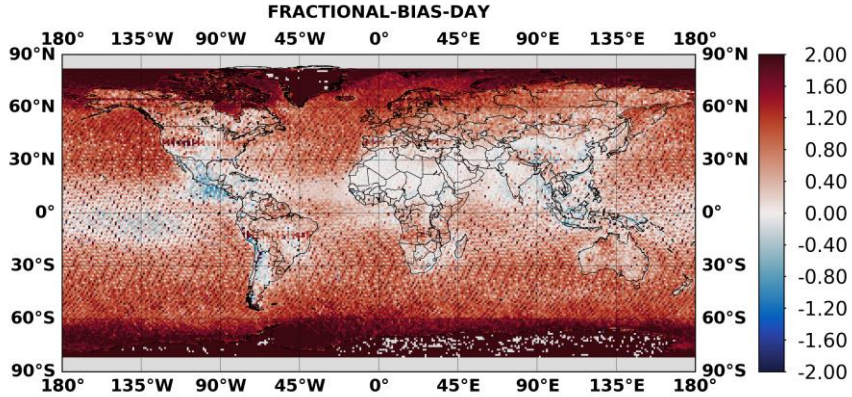
# Evaluation of MERRA-2 dust fraction versus LIVAS

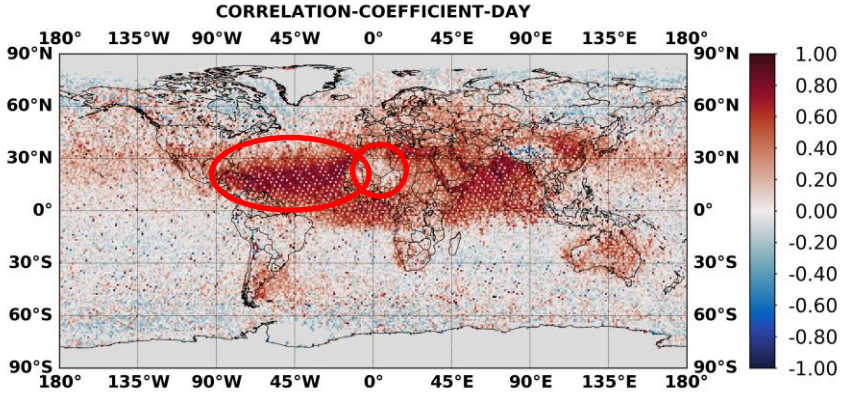
- Dust fraction derived from the LIVAS database (Amiridis et al., 2015)
- Highly accurate detection of depolarizing mineral particles ➔ dust separation from dusty mixtures
- Aggregation of quality-assured (Marinou et al., 2017) CALIOP L2 profiles (V3) at 1° x 1° spatial resolution
- Regionally-dependent dust lidar ratios instead of the universal value (40 sr)
- Use only of daytime CALIOP profiles (2007 – 2015)

## Global patterns

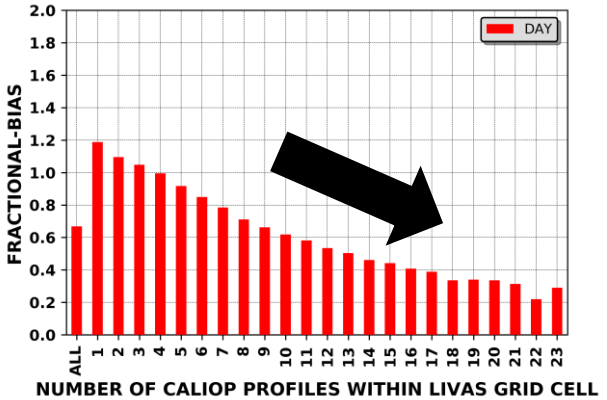


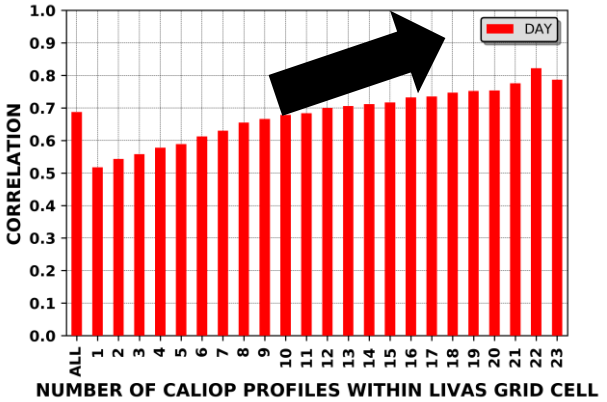




## Global metrics



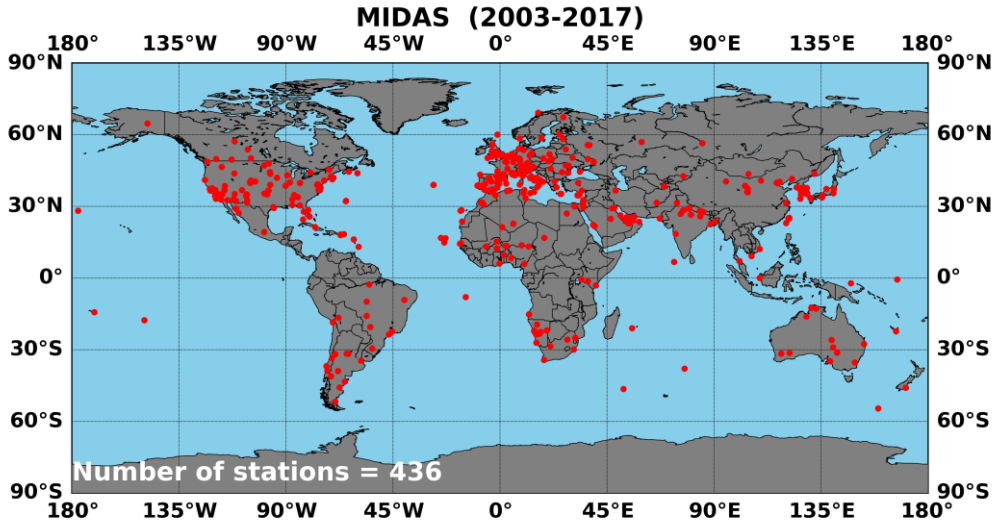
# Evaluation against AERONET (global metrics)

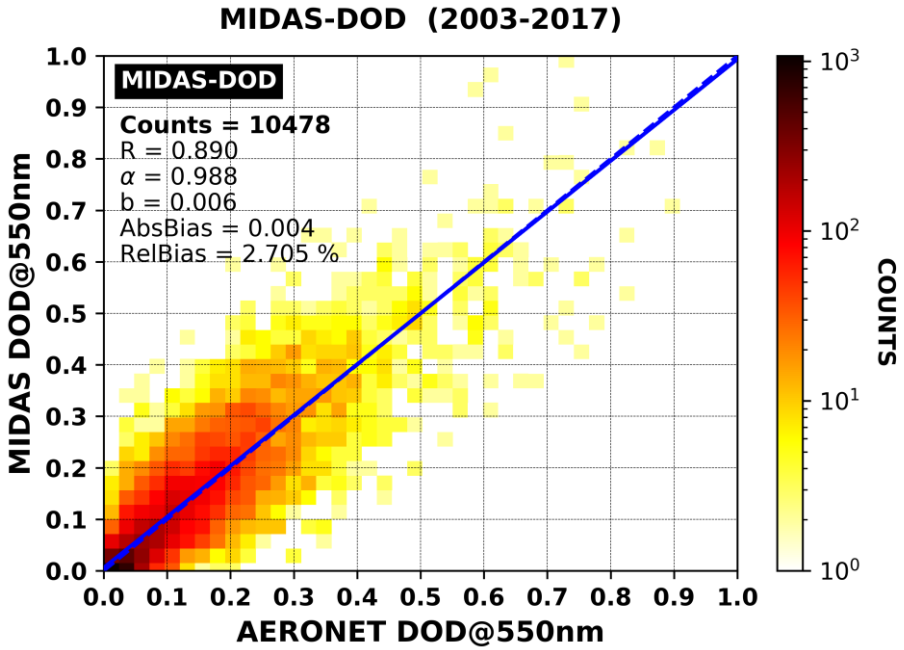
## AERONET data

- AERONET V3 (Giles et al., 2019) almucantar retrievals (Dubovik et al., 2006) – All points files
- Spectral AODs and Ångström exponent (440 – 870nm) – Level 2
- Spectral SSAs [Level 2 and Level 1.5]

## AERONET-derived DOD

- Selection of records when $\alpha_{440\text{-}870nm} \leq 0.75$ (predominance of coarse aerosols) and $SSA_{675nm} - SSA_{440nm} > 0$ (dust discrimination from sea-salt particles)
- SSA: decreasing absorptivity for increasing wavelengths in the visible spectrum in pure or dust-rich environments (Giles et al., 2012).
- From coarse AODs (440, 675 and 870nm) it is calculated the Ångström exponent in order to obtain the coarse AOD at 550nm which is considered as the **AERONET-derived DOD**
- Mitigation of non-dust aerosols' contribution to the columnar aerosol load
- Fine dust particles are ignored

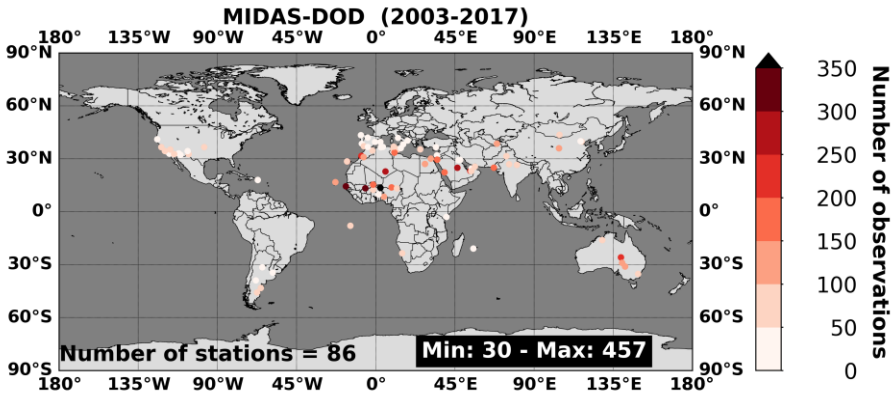


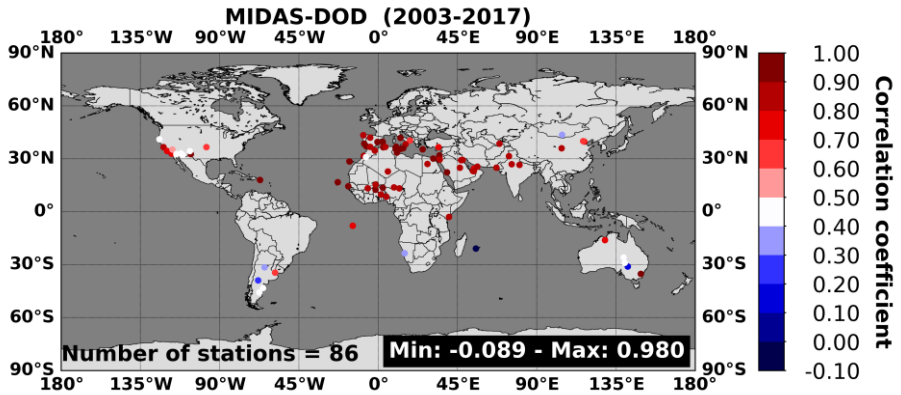
# Evaluation against AERONET (station level)

**Selection of sites with at least 30 matchups between ground-based and spaceborne DODs**

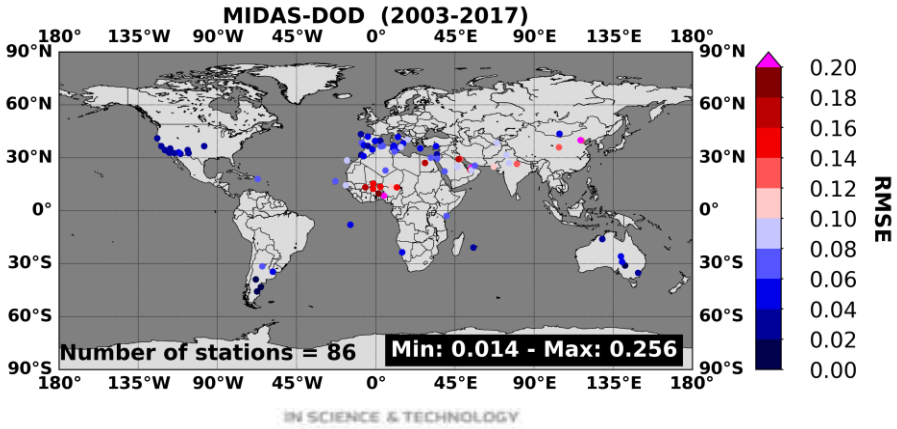
## Number of observations



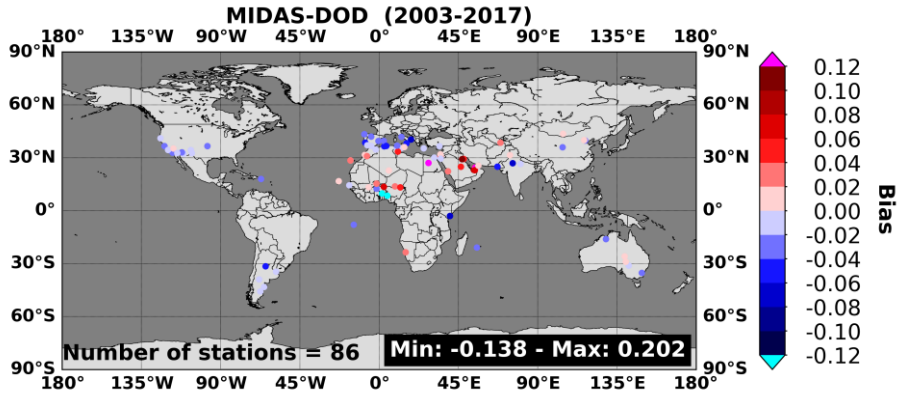

## Correlation coefficient




## Root-mean-square-error




## Bias



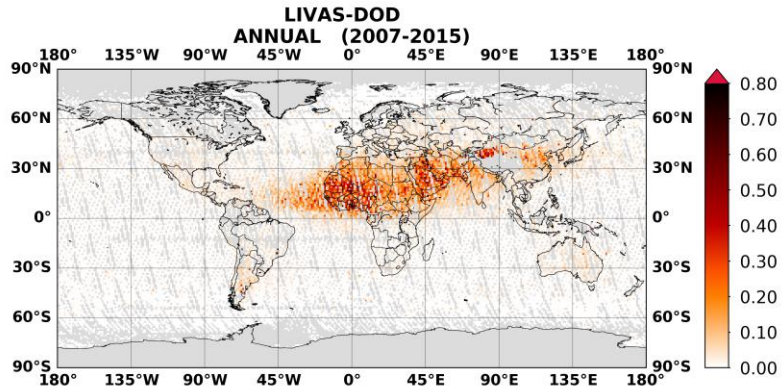

- Very high R values (>0.8) over sources and downwind regions
- Maximum RMSE levels in the sub-Sahel
- Mainly positive biases are recorded in the main dust sources of planet (fine dust particles are not taken into account in AERONET DODs)

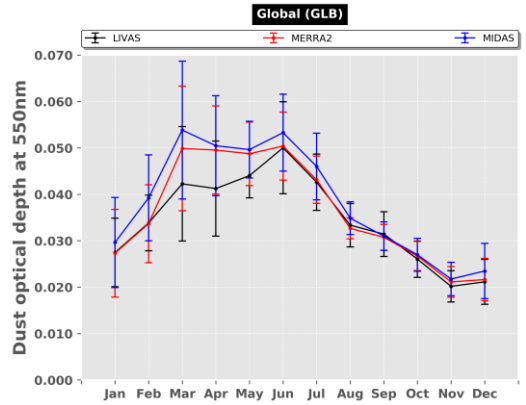
# Intercomparison of MIDAS, LIVAS and MERRA-2 DODs

## Geographical distributions

## Intra-annual variation

**LIVAS**

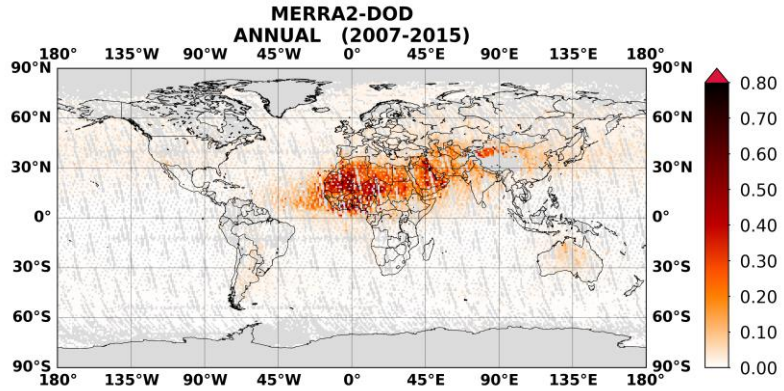


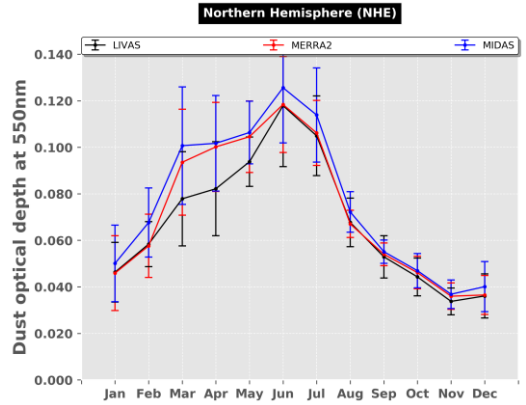




**Global**

**0.029 | 0.031 | 0.033**

**MERRA-2**

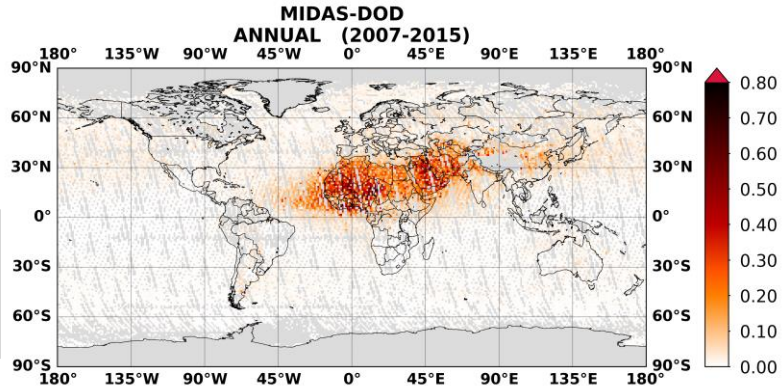


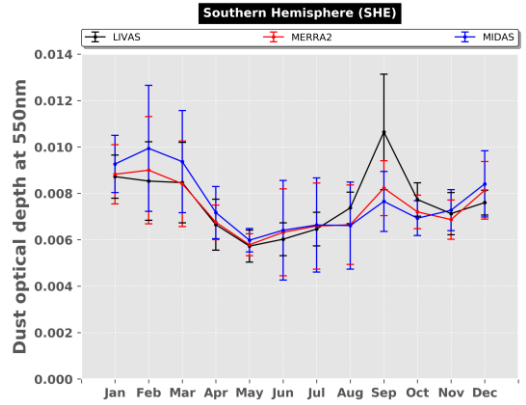




**N. Hemisphere**

**0.051 | 0.056 | 0.060**

**MIDAS**




**S. Hemisphere**

**0.008 | 0.008 | 0.008**

**2007-2015**
**1°x1°**

**LIVAS**
**MERRA-2**
**MIDAS**

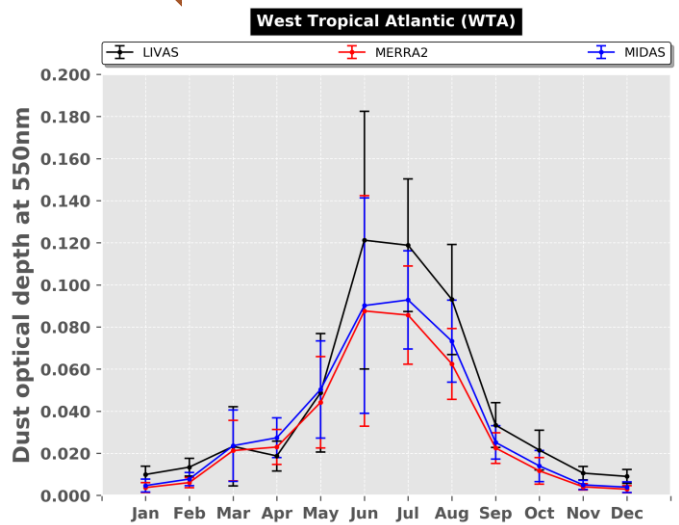
# Dust transport across Atlantic and Pacific

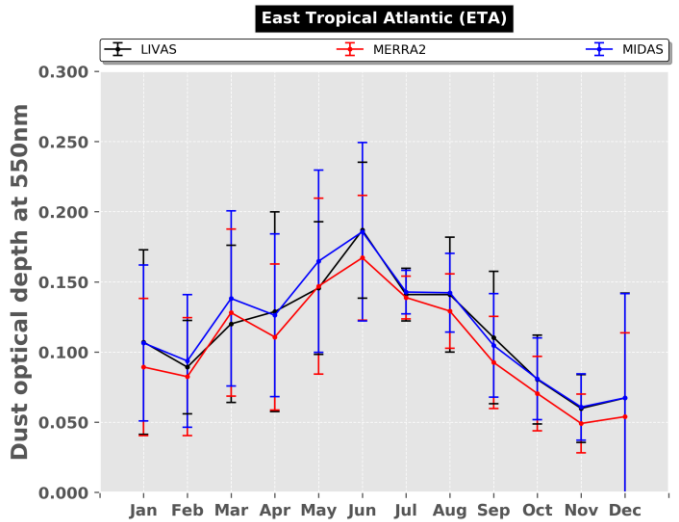
**Caribbean**

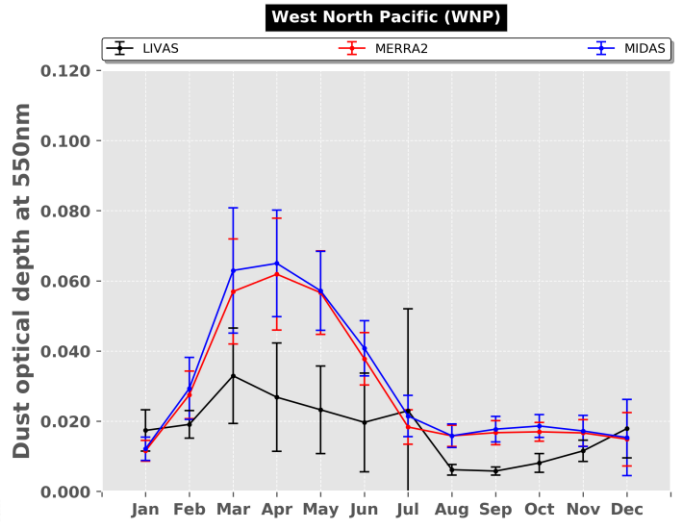
**Sahara**

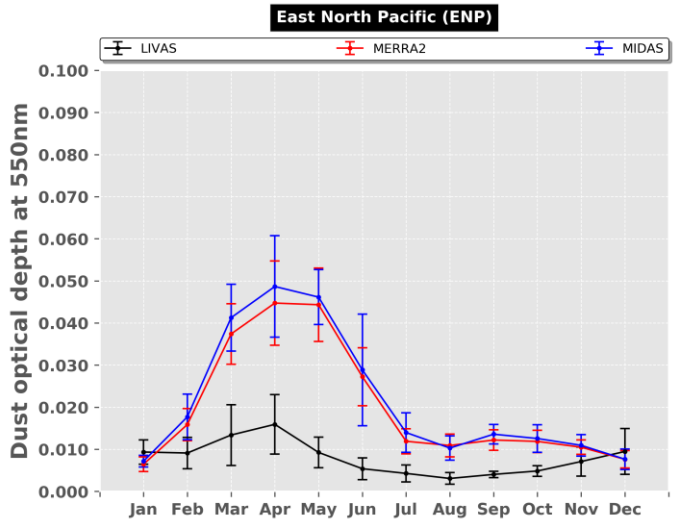
**Asia**

**US**




cost
EUROPEAN COOPERATION IN SCIENCE & TECHNOLOGY

# Uncertainty analysis

$$DOD_{MIDAS} = AOD_{MODIS} * MDF$$

$$\Delta(DOD) = \Delta(AOD) * MDF + AOD * \Delta(MDF)$$

$$\Delta(AOD_{DT-Ocean}) = \pm(0.10 * AOD + 0.04)$$

$$\Delta(AOD_{DT-Land}) = \pm(0.15 * AOD + 0.05)$$

$$\Delta(AOD_{DB-Land}) = \pm\left(\frac{a + b * AOD}{AMF}\right)$$

$$\Delta(AOD_{DTDB-Land}) = \pm\frac{\sqrt{[\Delta(AOD_{DT-Land})]^2 + [\Delta(AOD_{DB-Land})]^2}}{2}$$

- AOD is treated as prognostic uncertainty instead of diagnostic for the Dark Target (DT) algorithms
- AMF ➔ Air mass factor (Sayer et al., 2013) for the Deep Blue (DB) algorithm
- $a$ and $b$ coefficients depend on the underlying surface type (vegetated or arid based on the IGBP database)

$$\Delta(MDF) = \pm(2.282 * MDF^4 - 6.222 * MDF^3 + 4.700 * MDF^2 - 0.969 * MDF + 0.199)$$

- Utilization of the LIVAS dust fraction as reference

**Time dimension**

$$ME = \frac{\sqrt{\Delta(DOD)_1^2 + \cdots + \Delta(DOD)_N^2}}{N}$$

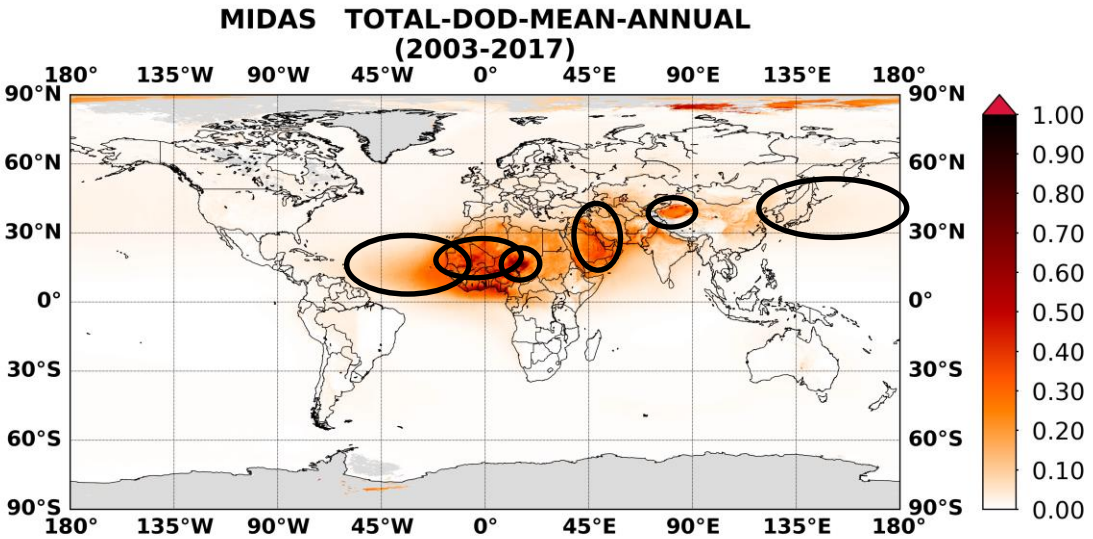
$$SE = \frac{SD}{\sqrt{N}}$$

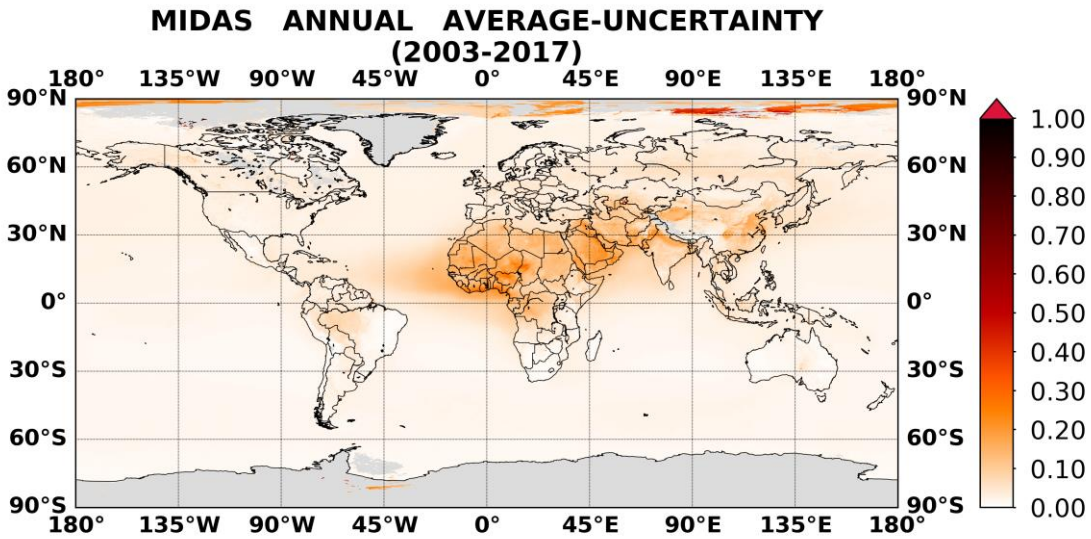
$$TE = \sqrt{ME^2 + SE^2}$$

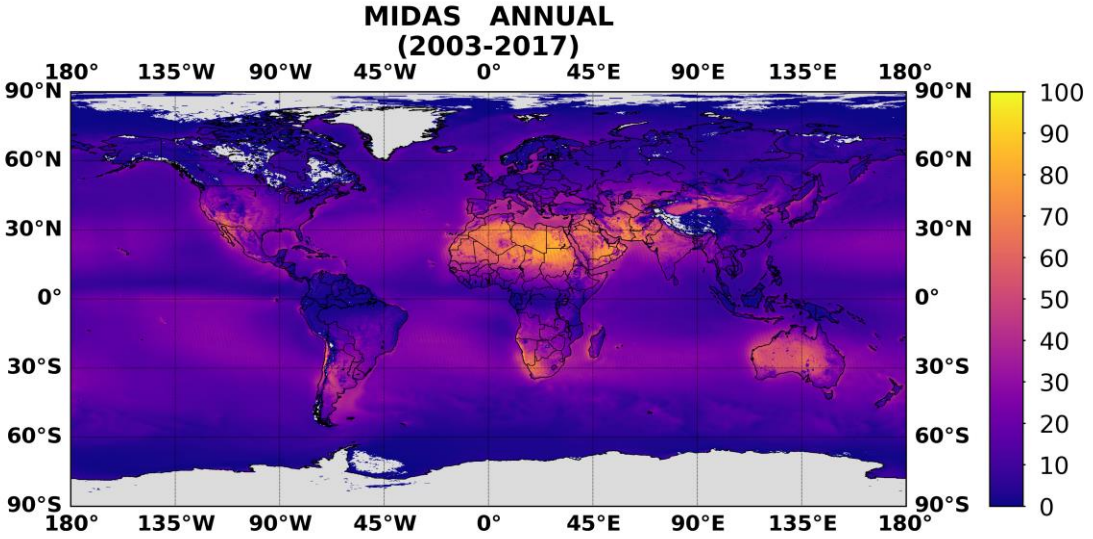
**Space dimension**

$$RE = \sum_{i=1}^{N} w_i * TE_i$$

# MIDAS DOD annual global patterns

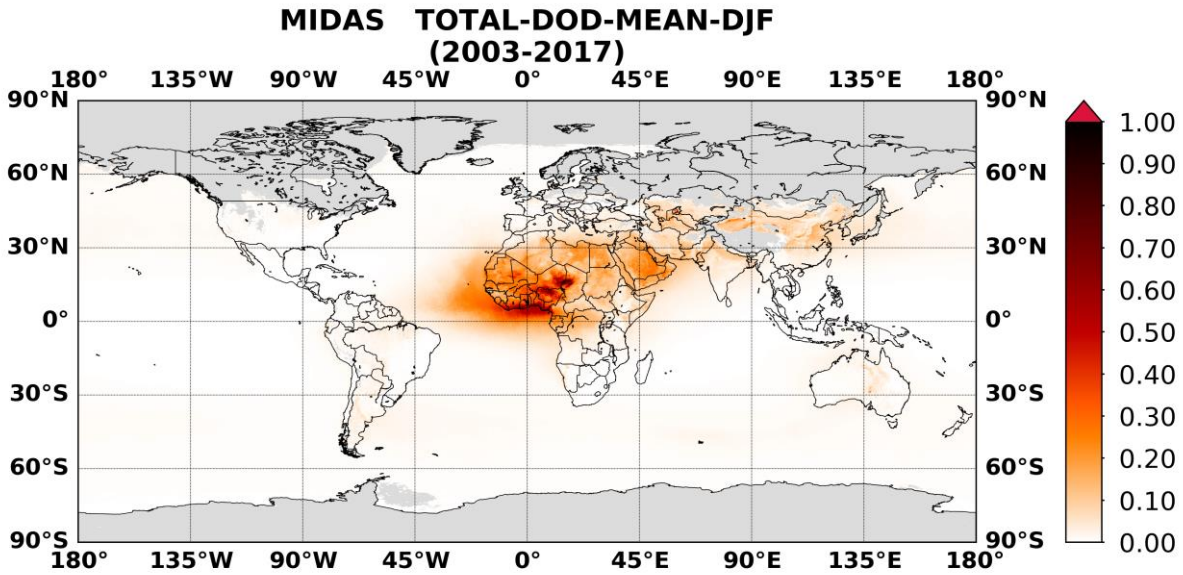


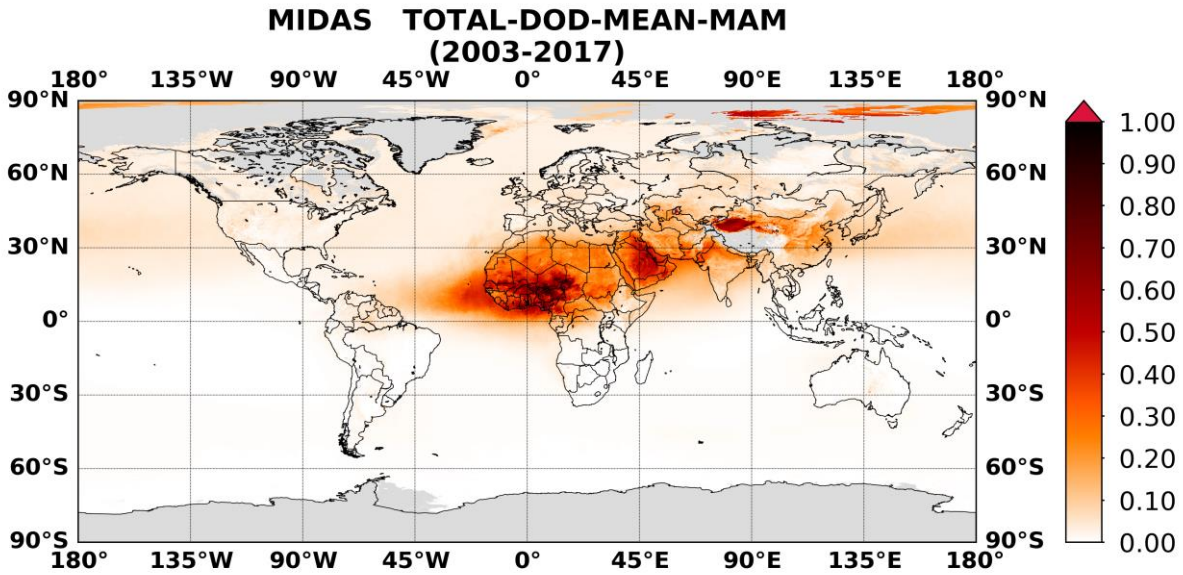



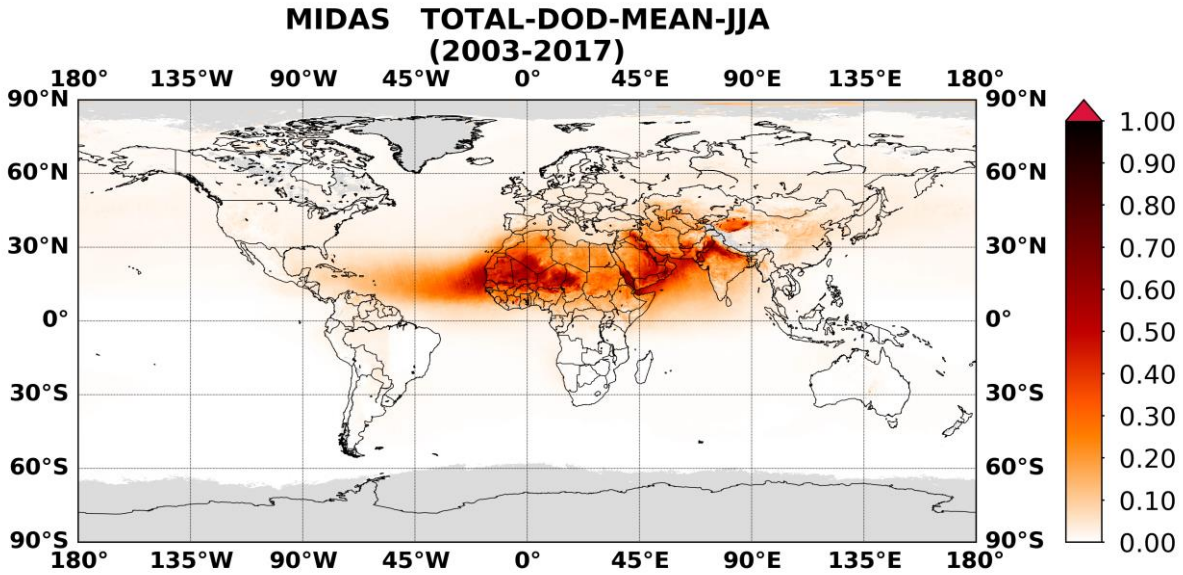



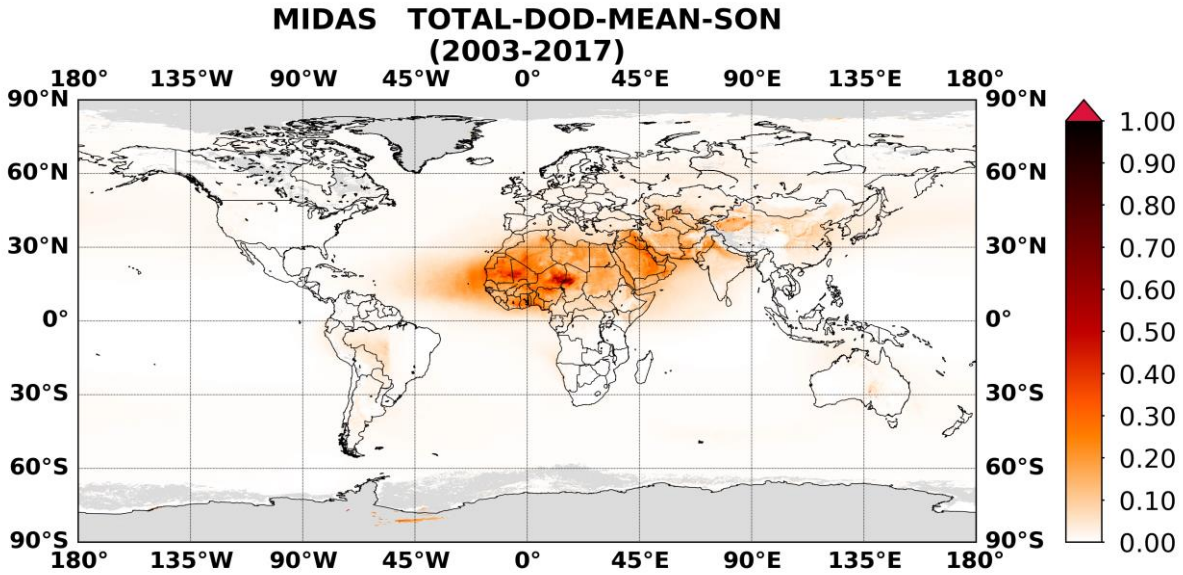

- Maximum DODs up to ~1.2 in the Bodélé Depression (northern Lake Chad)
- Moderate-to-high DODs are recorded in the W. Sahara, Middle East and the Taklamakan Desert
- Dust transport over the Atlantic and Pacific Oceans
- Average of DOD uncertainties (up to 0.5) scales with DOD
- MIDAS DOD availability is higher than 70% in areas less affected by clouds

# MIDAS DOD seasonal global patterns



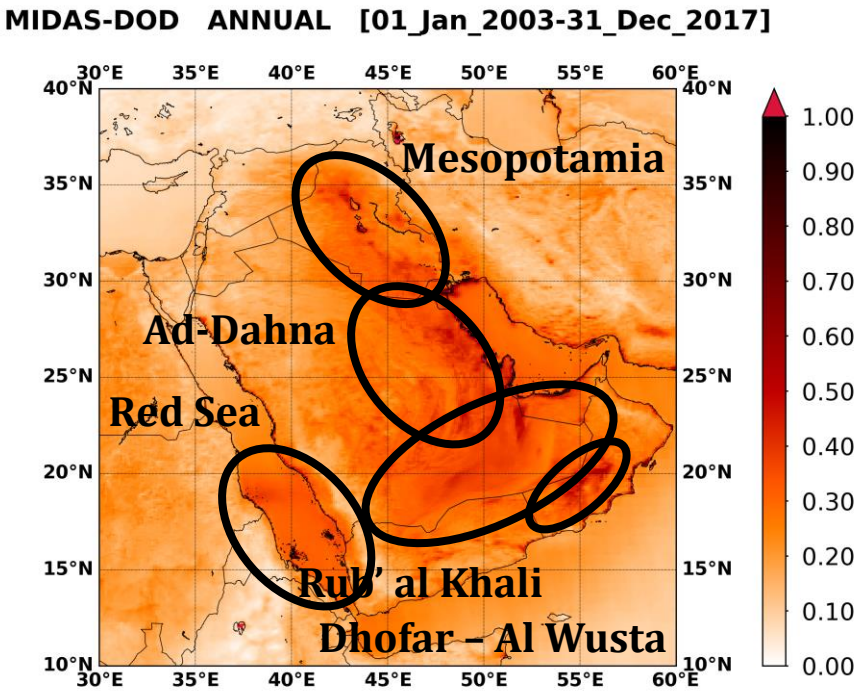



# Climatology and trends

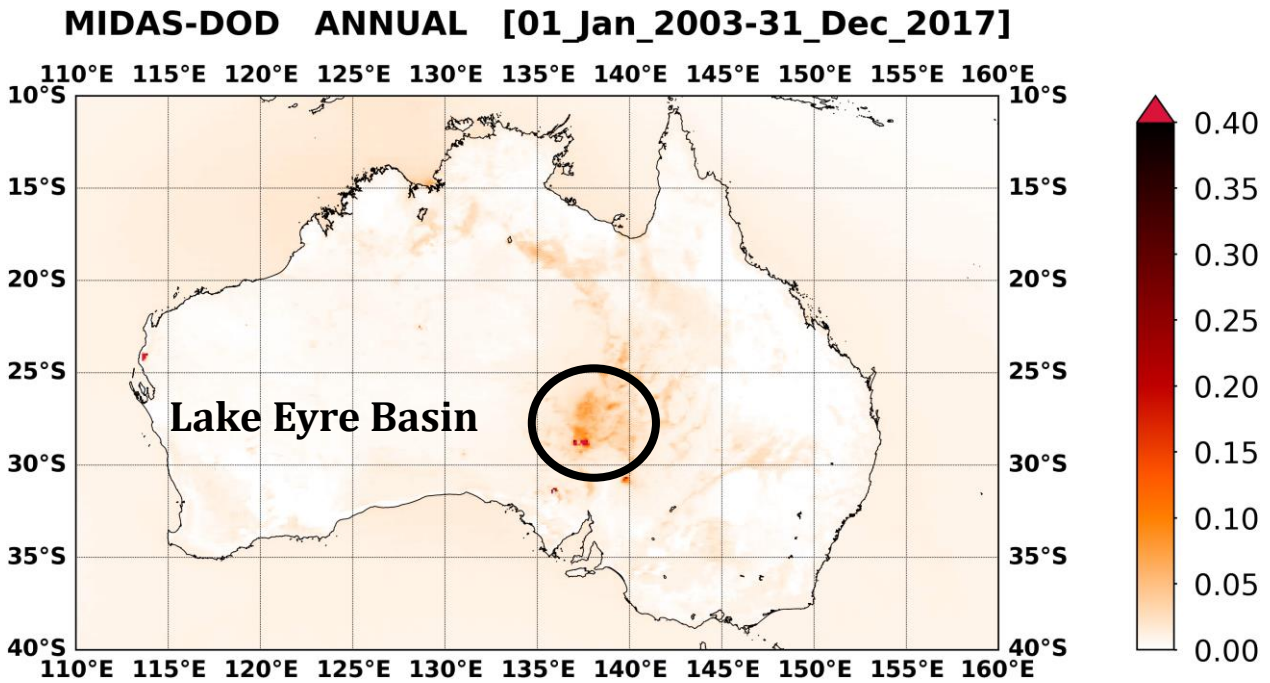
cost
EUROPEAN COOPERATION
IN SCIENCE & TECHNOLOGY

# Focus on dust sources and downwind areas

## Middle East




## Australia




**Description of dust aerosols' regime in 9 regions of the planet encompassing the major sources and areas subjected to dust transport**

cost EUROPEAN COOPERATION IN SCIENCE & TECHNOLOGY



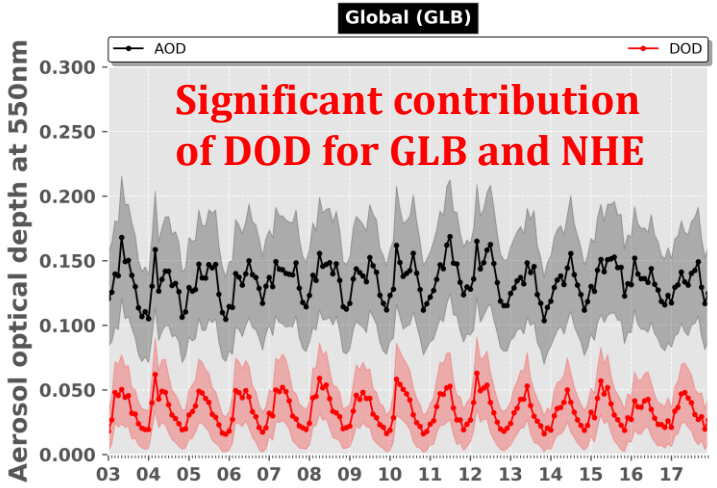
Gkikas et al. (in preparation)

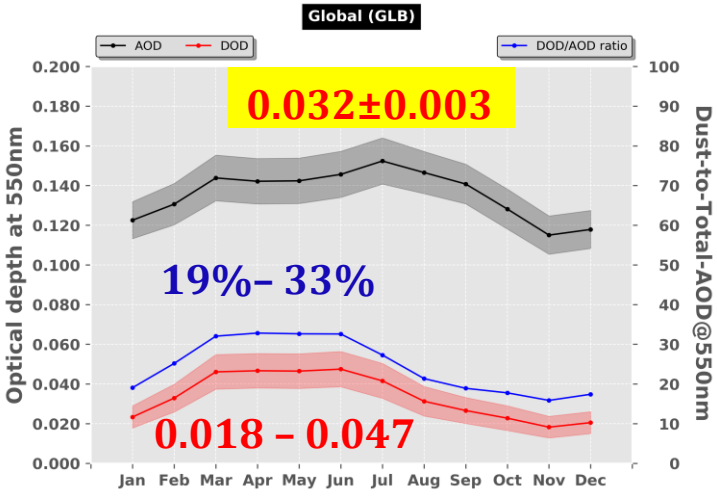
# Temporal variation of global and hemispherical averages

Interannual

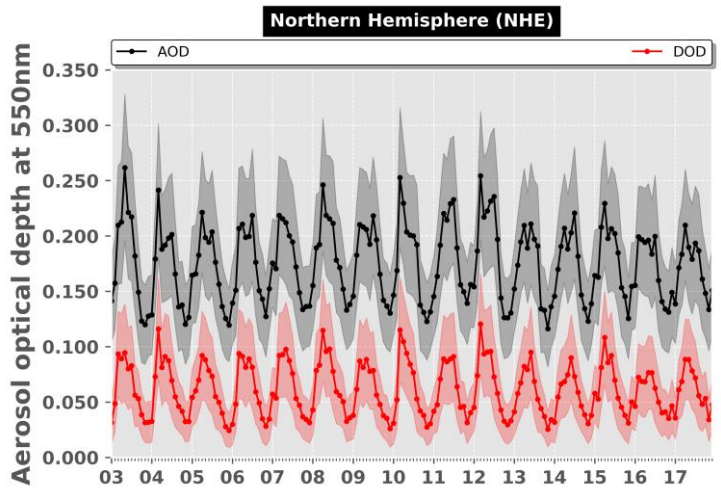
Intra-annual

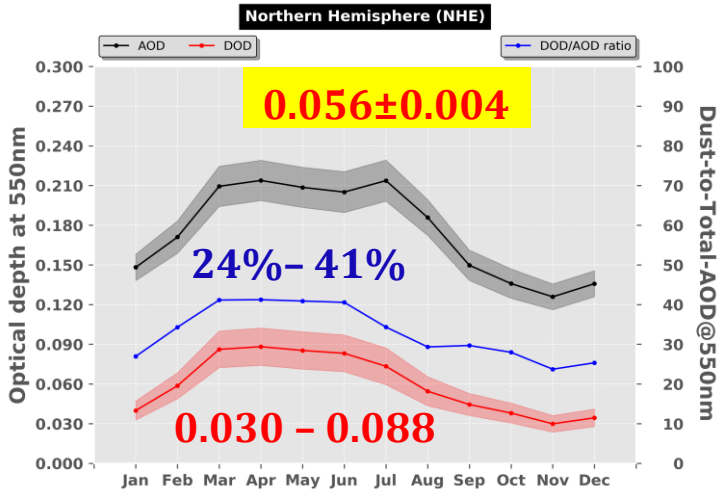
## Global



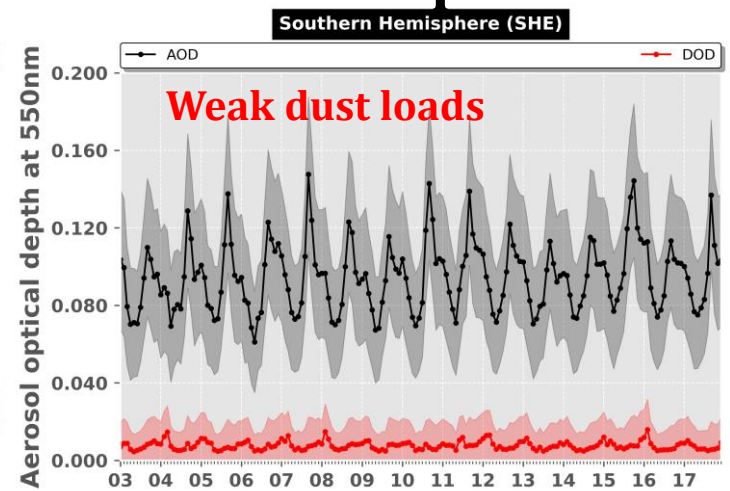



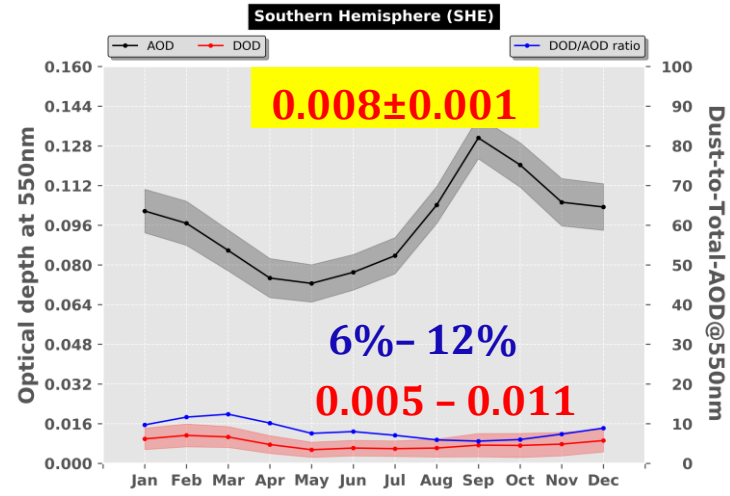

## N. Hemisphere




## S. Hemisphere



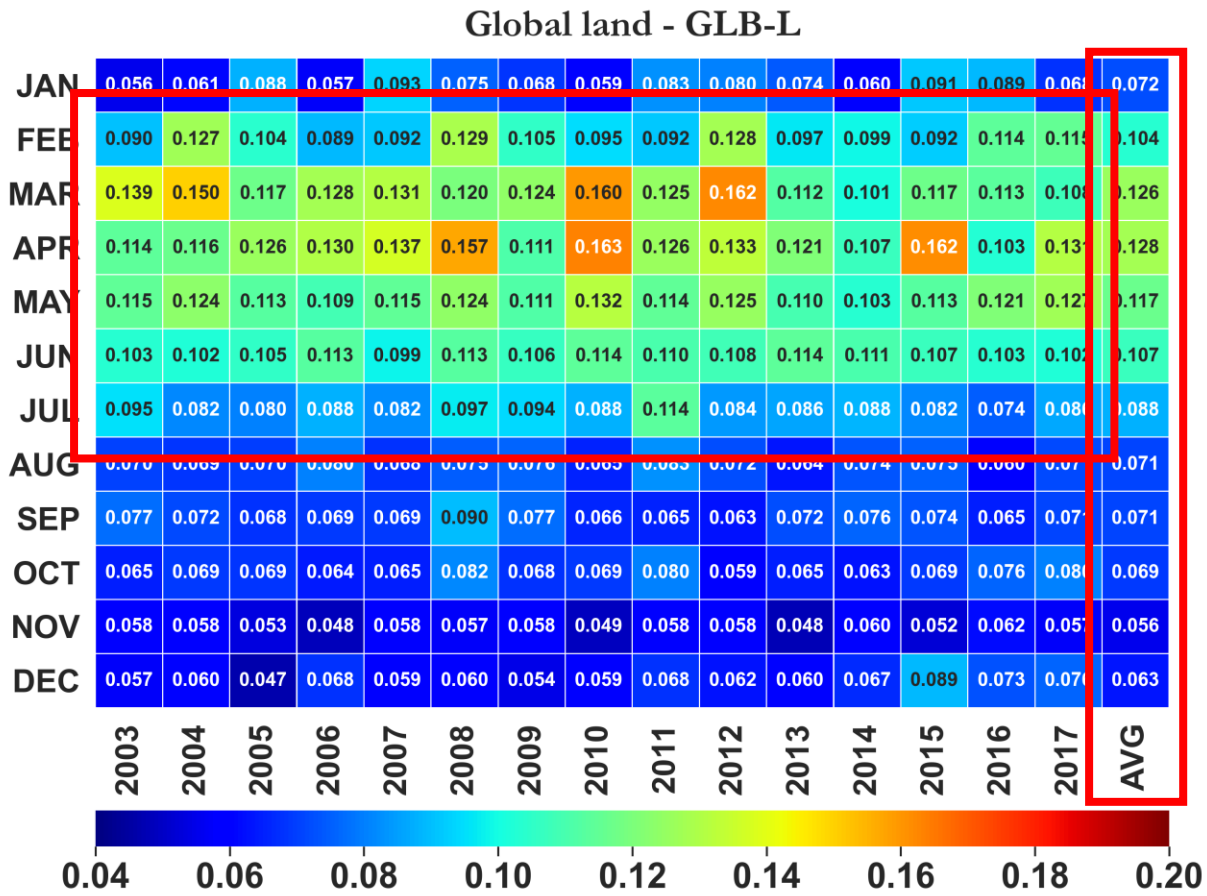



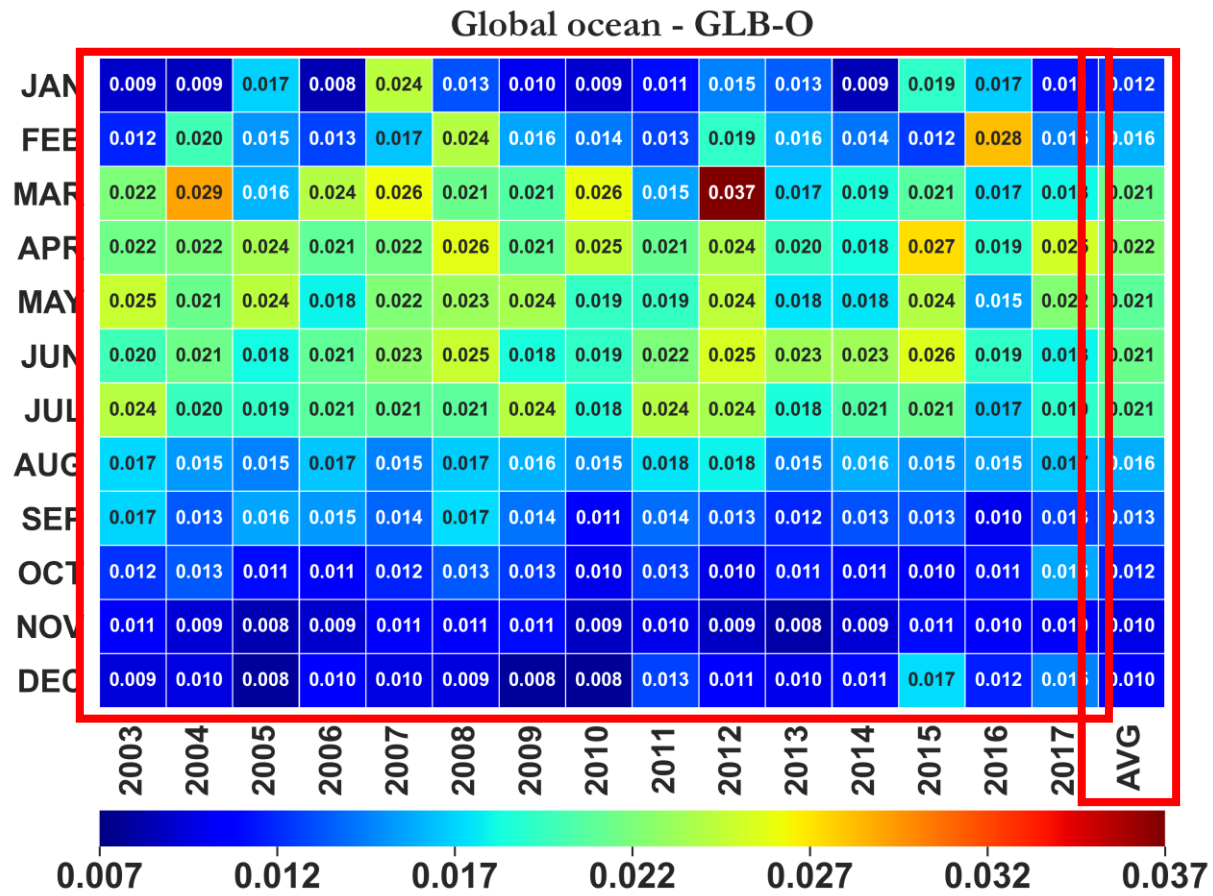

**AOD | DOD | DOD-AOD ratio**



Gkikas et al. (in preparation)

# Dust seasonal cycles over land and ocean

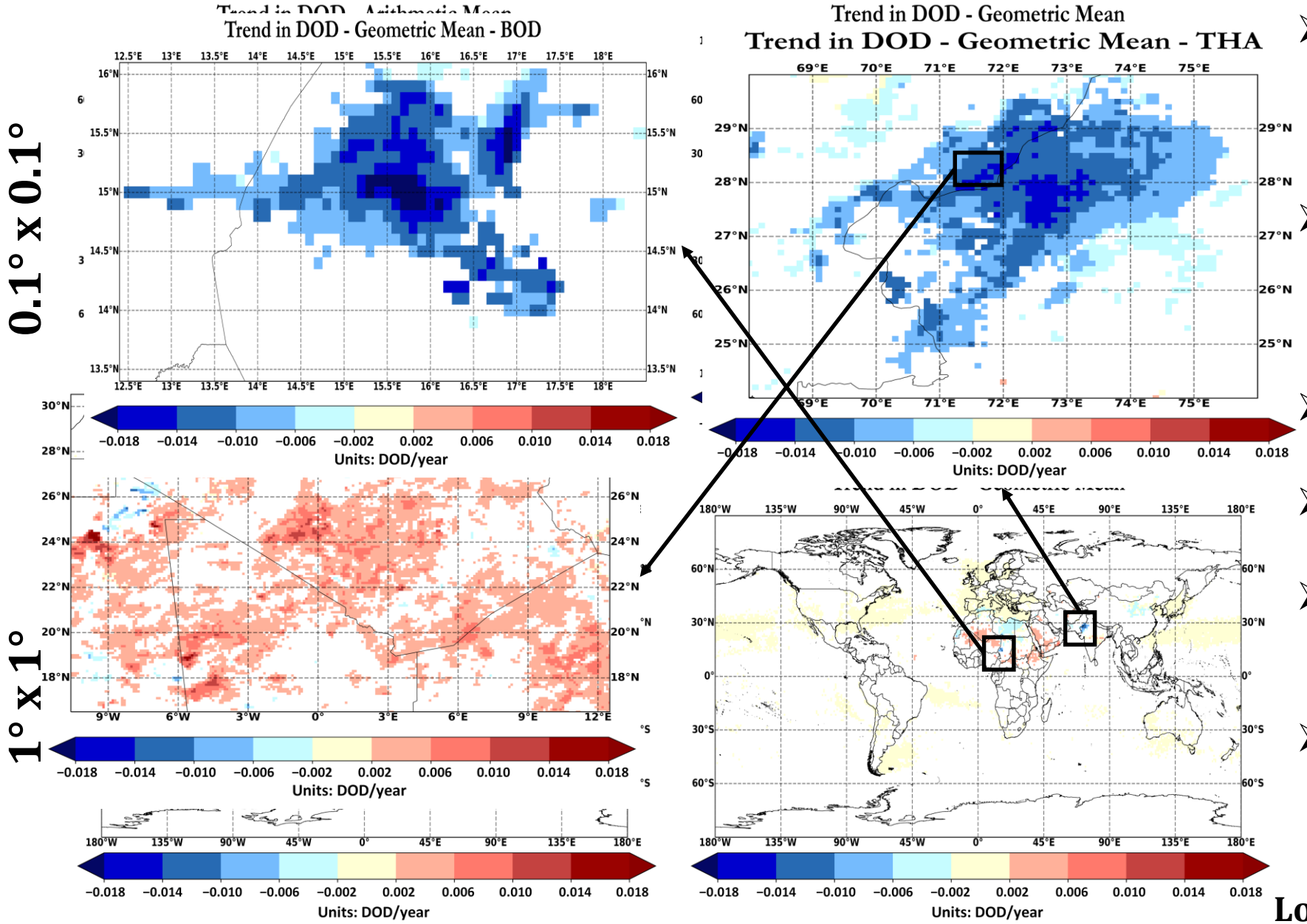



- Strong year-by-year DOD variations, over land, during the high-dust months (Feb – Jul)
- Rather stable DOD seasonal cycles over oceans throughout the MIDAS temporal coverage (2003-2017)
- **Land:** 0.056 – 0.128
- **Ocean:** 0.010 – 0.022

**Logothetis et al. (in preparation)**

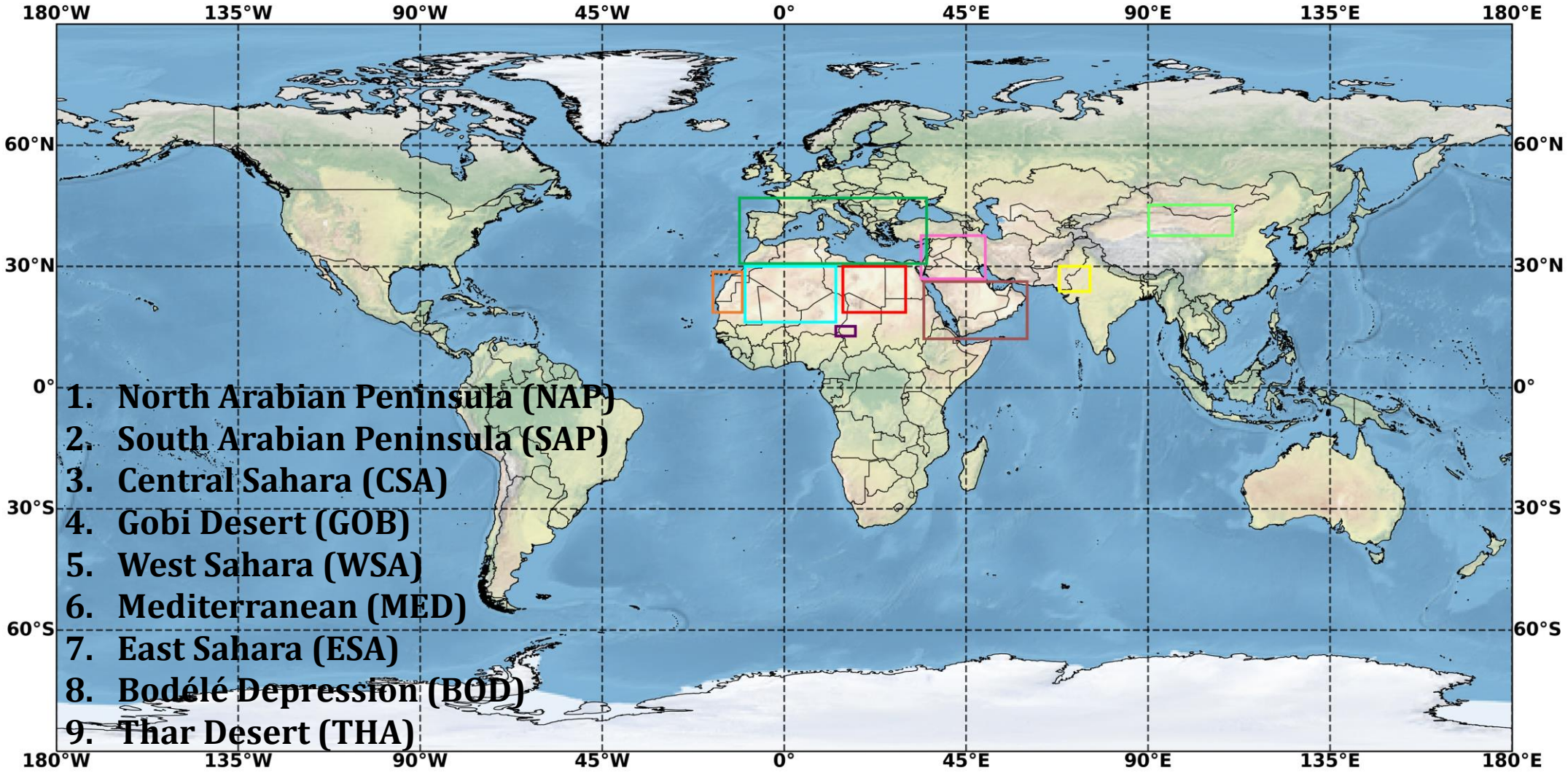
# Trends of dust burden over the period 2003 – 2017




- Calculation of monthly arithmetic and geometric averages when at least 6 days are available at each grid-cell
- Trends of deseasonalized DODs when at least 5 out of 15 years are available (Hsu et al., 2012)
- 95% confidence level (Weatherhead et al., 1998)
- Maximum **positive trends** in the western part of Sahara
- Maximum **negative trends** in the Bodélé and the Thar Desert
- **Contributing factors on the obtained DOD trends (ongoing work)**

**Logothetis et al. (in preparation)**

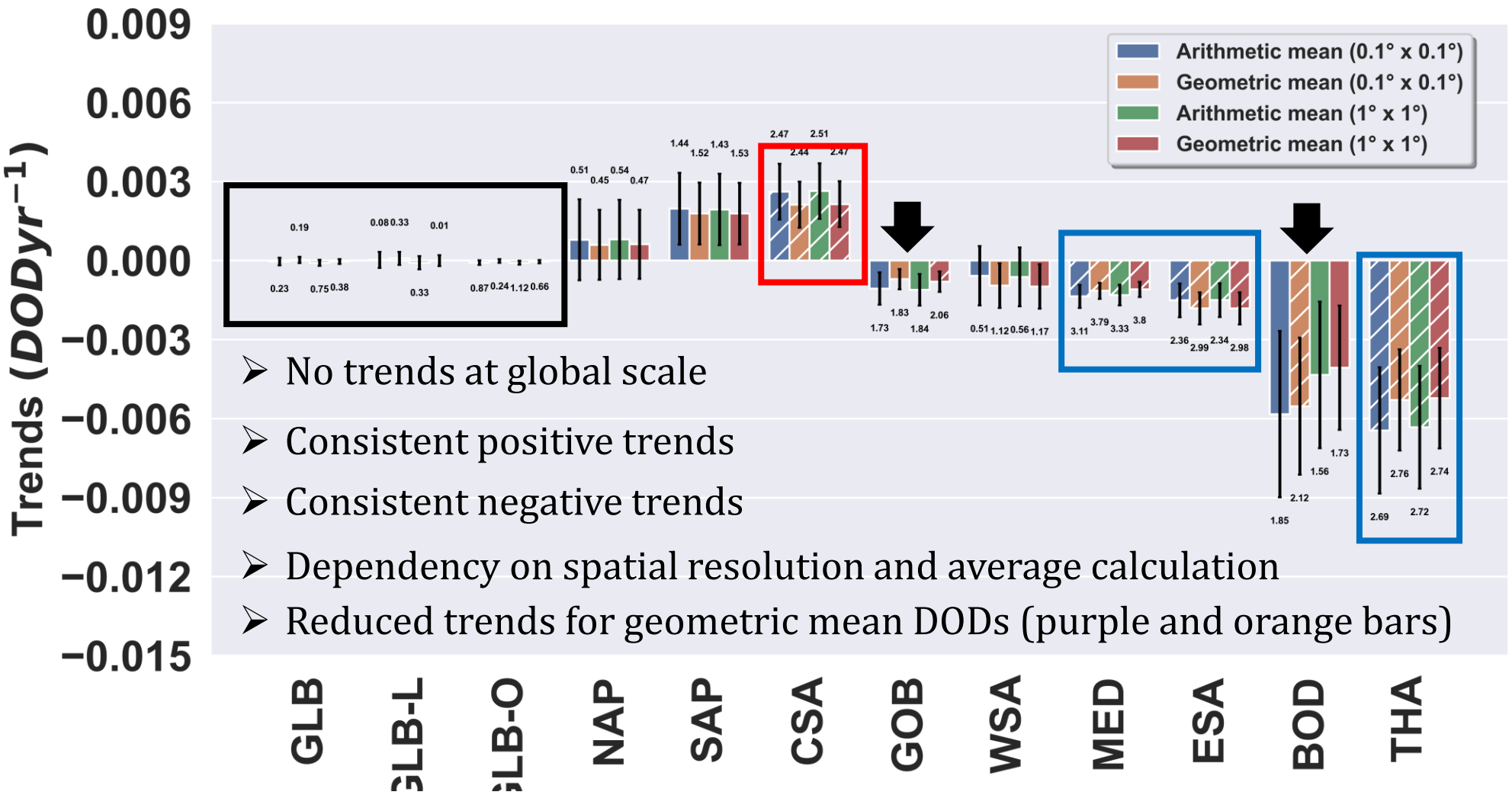
# Domains of interest






Logothetis et al. (in preparation)

# Global and regional DOD trends (2003 – 2017)




- No trends at global scale
- Consistent positive trends
- Consistent negative trends
- Dependency on spatial resolution and average calculation
- Reduced trends for geometric mean DODs (purple and orange bars)

- Numbers above bars: $|\omega/\sigma_\omega| > 2$ (95% confidence level)
- Error
- Hatched bars: statistical significant trends

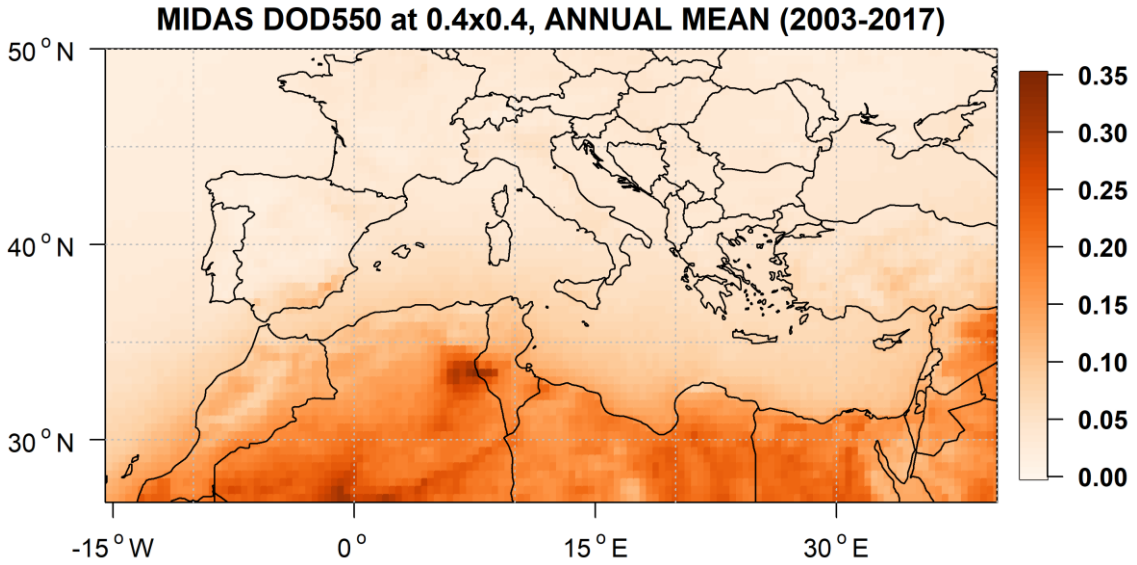


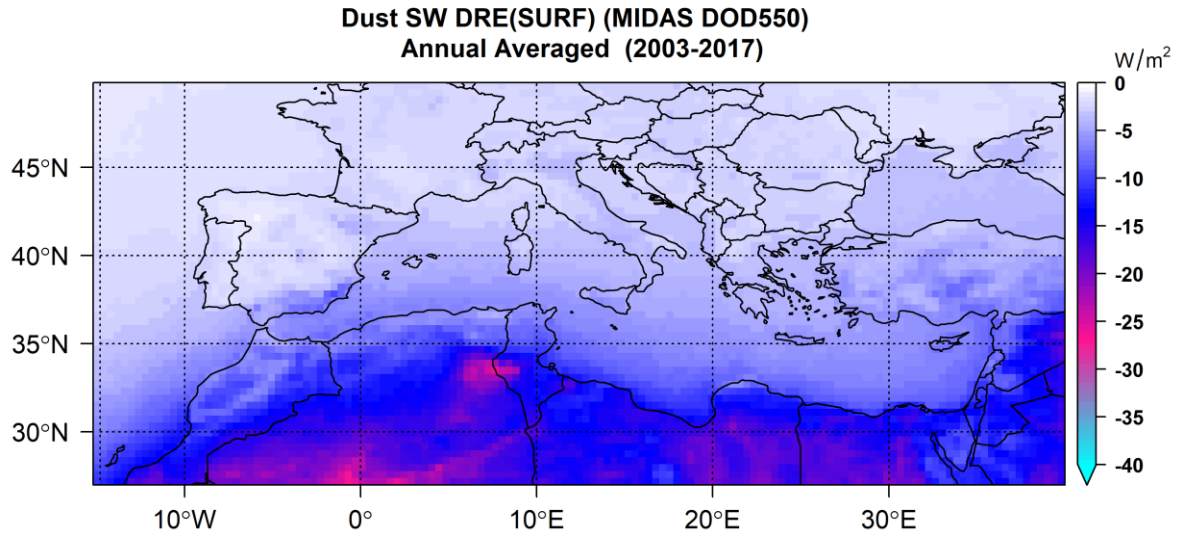
**Logothetis et al. (in preparation)**

# Radiative effects

cost
EUROPEAN COOPERATION
IN SCIENCE & TECHNOLOGY

# Perturbation on the downward SW radiation at the ground




- Dust-induced perturbations on the downwelling SW radiation at the surface under clear-sky conditions
- Impacts on solar energy production
- The broader Mediterranean basin is frequently affected by mineral particles originating primarily in the Sahara Desert and secondarily in the Middle East
- The spatial patterns of DREs are driven by those of dust optical depth
- Distinct south-to-north gradient of the surface SW DREs

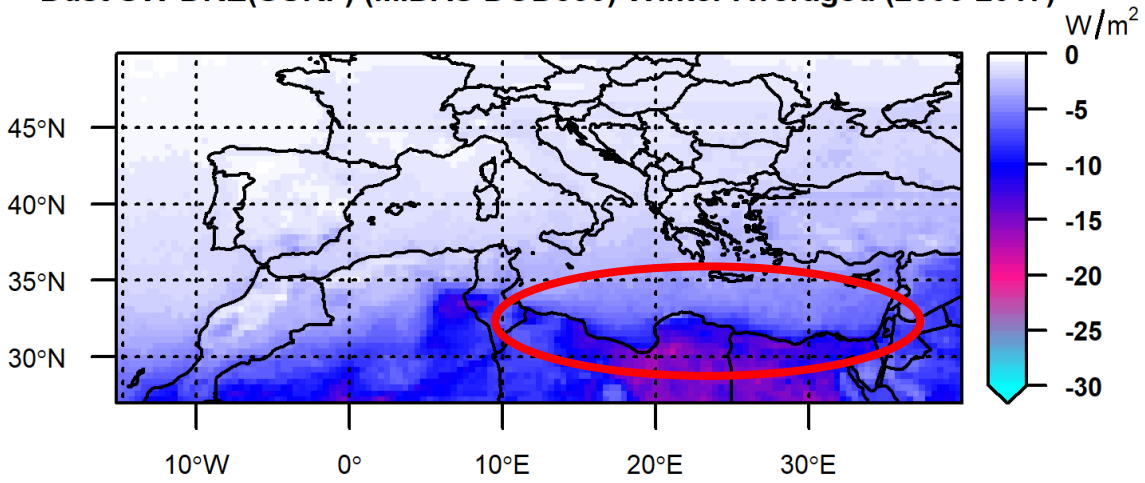
cost
EUROPEAN COOPERATION IN SCIENCE & TECHNOLOGY



**Papachristopoulou et al. (in preparation)**

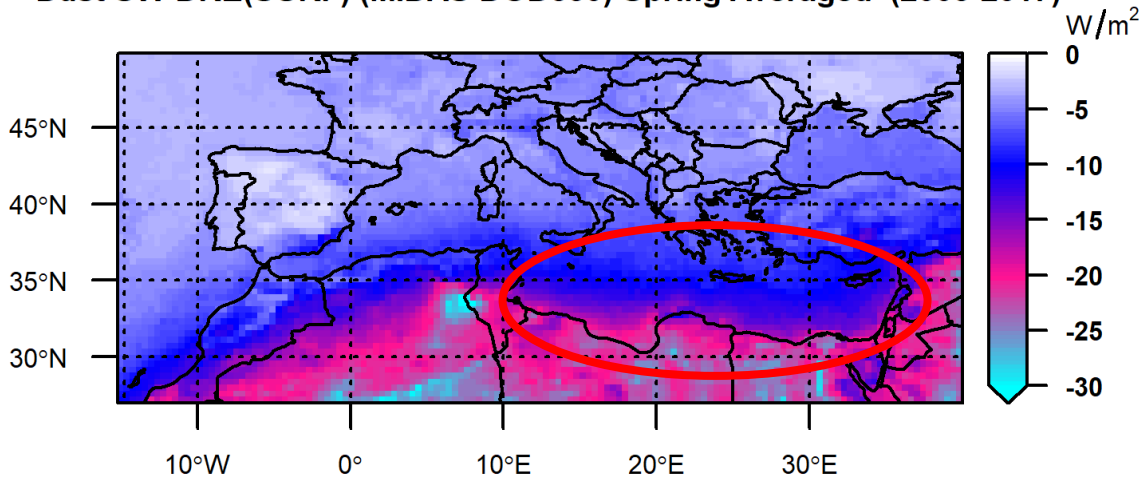
# Seasonal variability of the surface SW DREs

Dust SW DRE(SURF) (MIDAS DOD550) Winter Averaged (2003-2017)



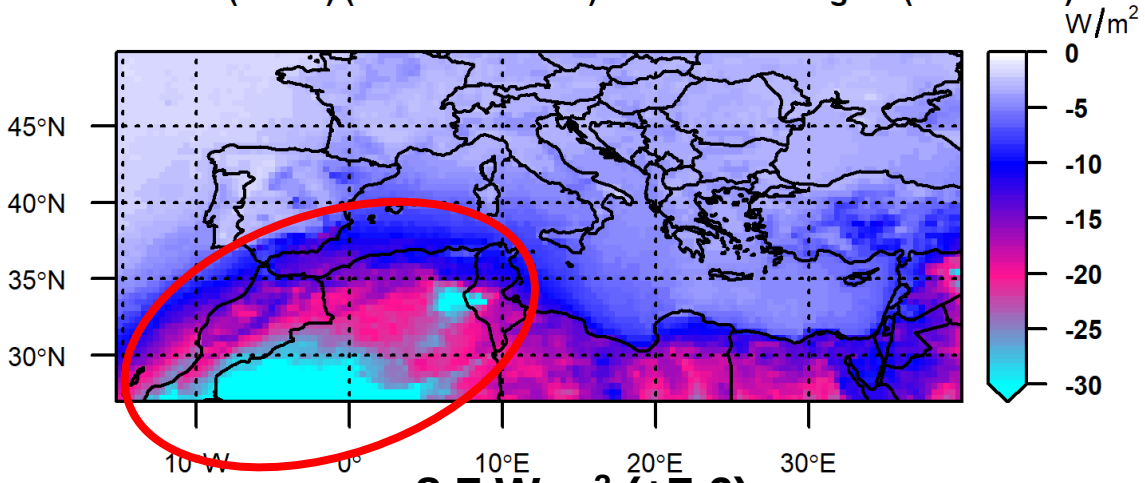

**-3.6 Wm$^{-2}$ (±3.7)**

Dust SW DRE(SURF) (MIDAS DOD550) Spring Averaged (2003-2017)



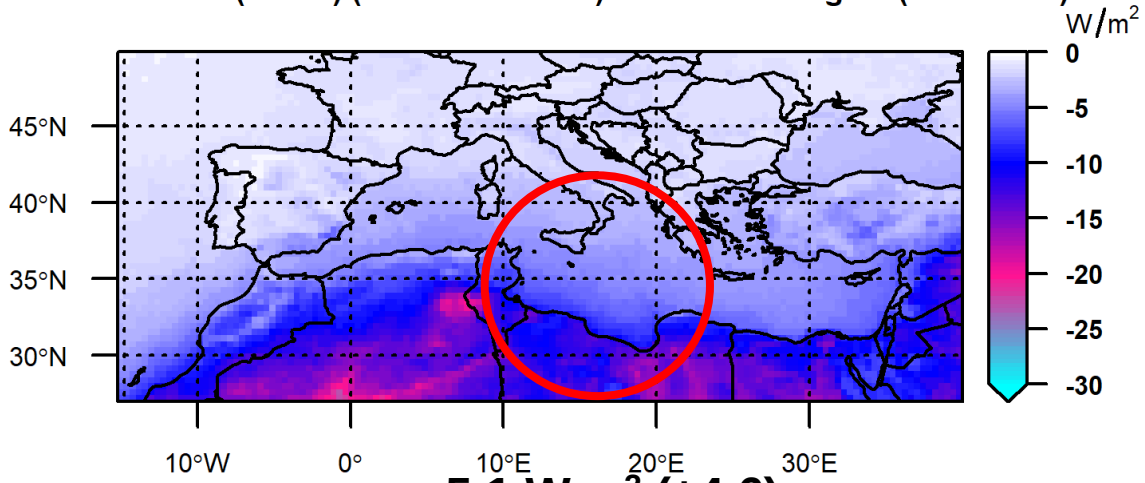

**-9.4 Wm$^{-2}$ (±7.0)**

Dust SW DRE(SURF) (MIDAS DOD550) Summer Averaged (2003-2017)




**-8.7 Wm$^{-2}$ (±7.6)**

Dust SW DRE(SURF) (MIDAS DOD550) Autumn Averaged (2003-2017)



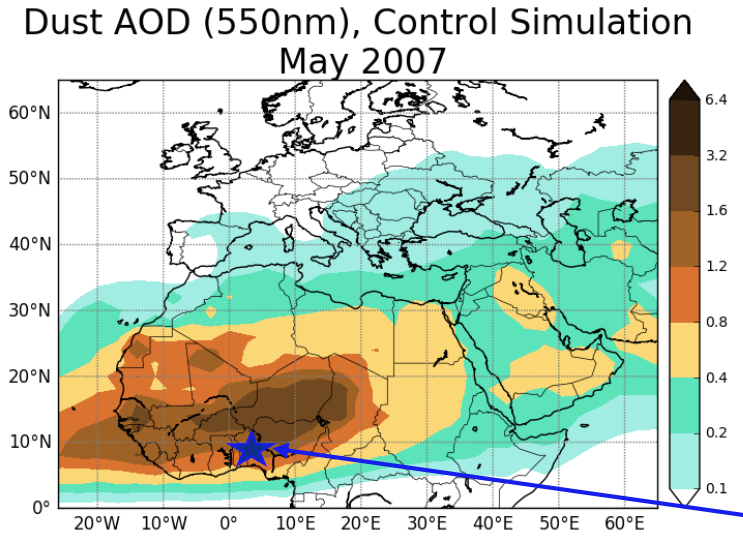

**-5.1 Wm$^{-2}$ (±4.6)**

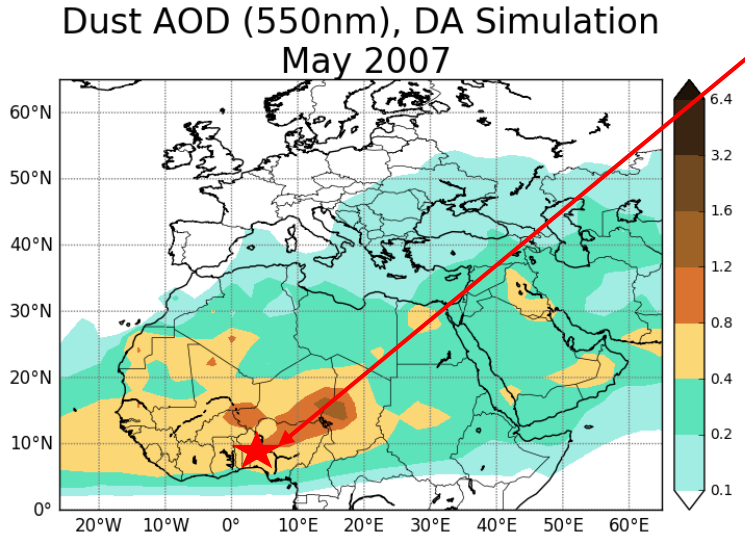
**Papachristopoulou et al. (in preparation)**

# Data assimilation

cost
EUROPEAN COOPERATION
IN SCIENCE & TECHNOLOGY

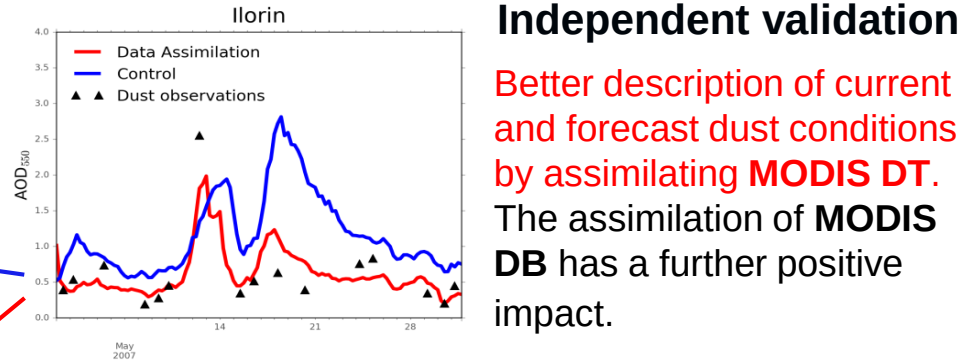
# MIDAS assimilation in the MONARCH model




**Enza Di Tomaso**
**Carlos Pérez García-Pando**

**Control | DA | Observations**




**Independent validation**

Better description of current and forecast dust conditions by assimilating **MODIS DT**. The assimilation of **MODIS DB** has a further positive impact.

*Reference data set: AERONET dust-filtered observations (not assimilated)*

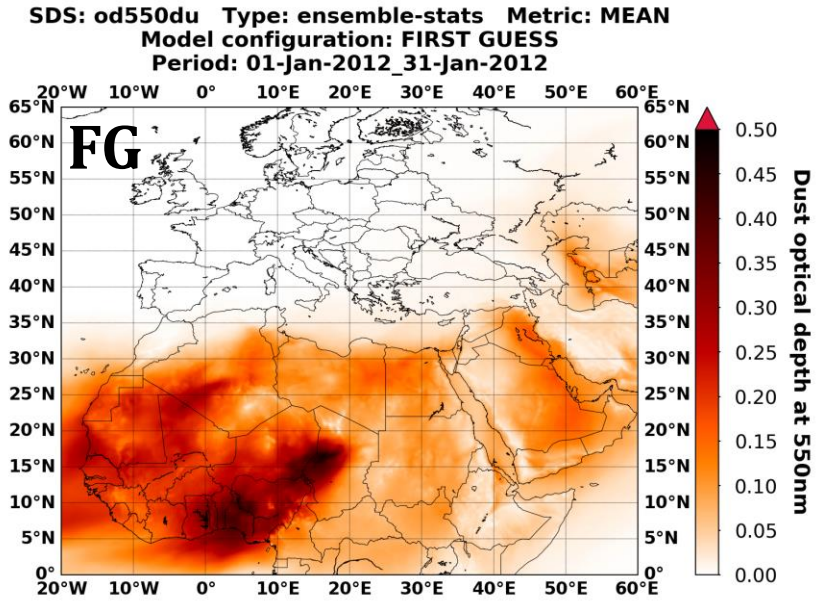
*Di Tomaso et al. (2017)*

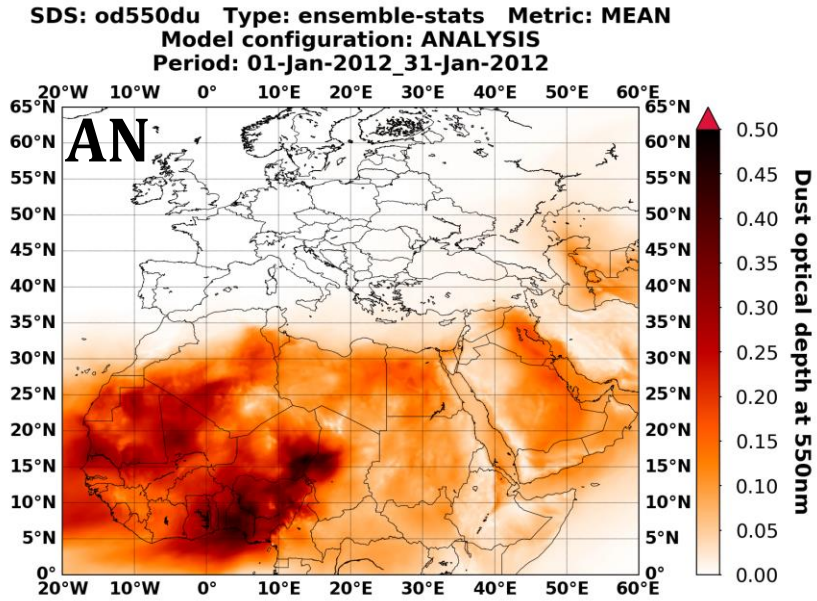
**MIDAS provides an improved data set for data assimilation applications**

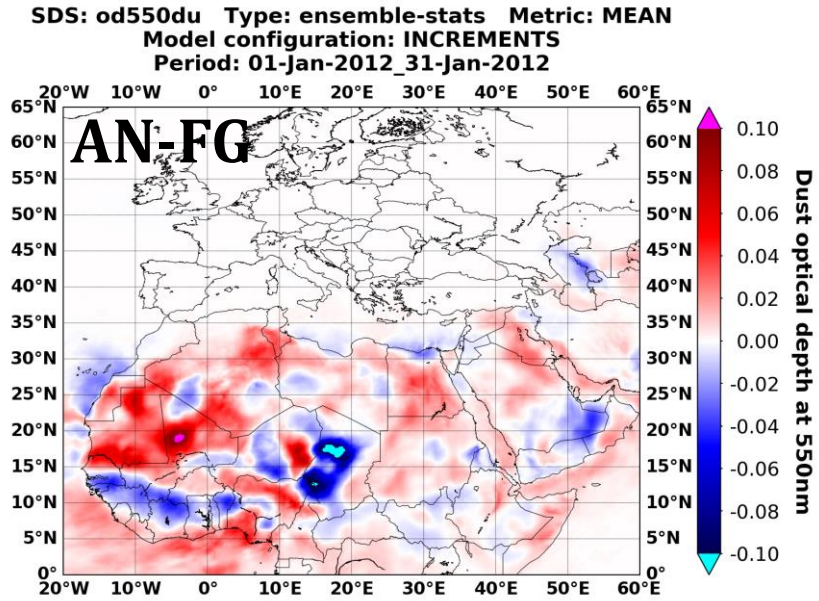
## MIDAS

- MONARCH ensemble simulations. First tested configuration:
  - 12-member ensemble
  - 2 datasets of initial and boundary conditions (ERAinterim, MERRA-2 with ERA5soil)
  - 2 dust emission schemes (Pérez et al., 2011; Ginoux et al., 2001)
  - Random perturbations on emission dust size distribution at sources and friction velocity threshold

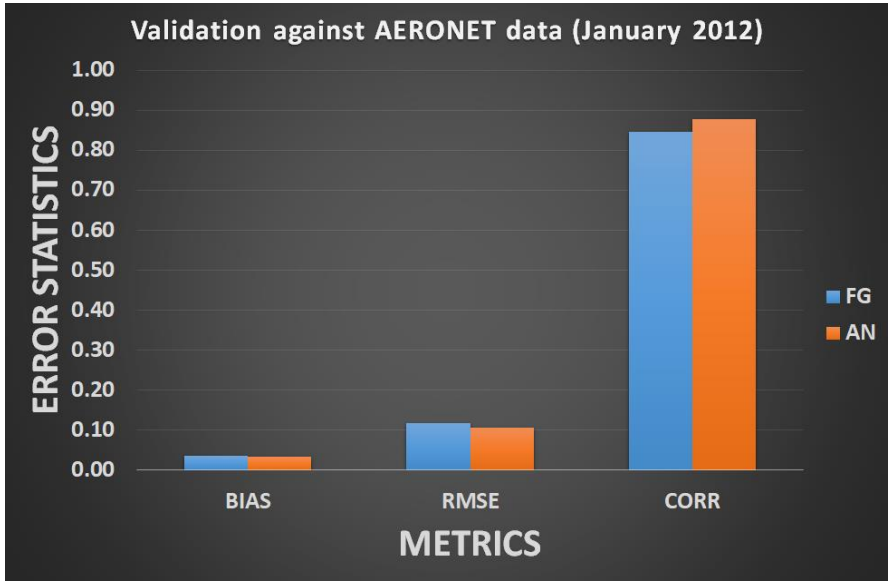
# MIDAS assimilation: first test (January 2012)




**Evaluation against AERONET SDA retrievals**

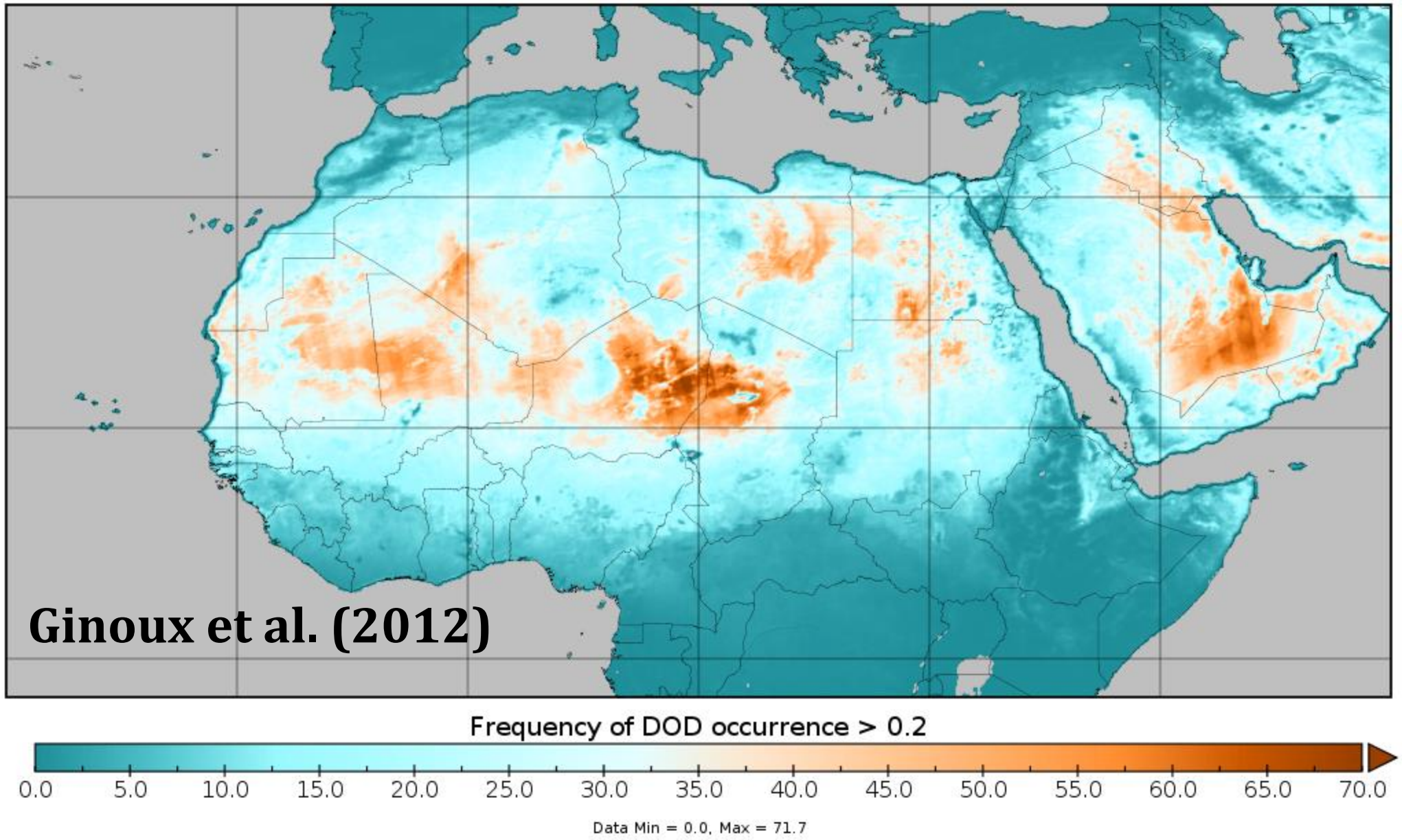



**Better evaluation metrics for the analysis compared to the first-guess (i.e., an analysis-initialized forecast)**

# Dust sources identification

cost
EUROPEAN COOPERATION
IN SCIENCE & TECHNOLOGY

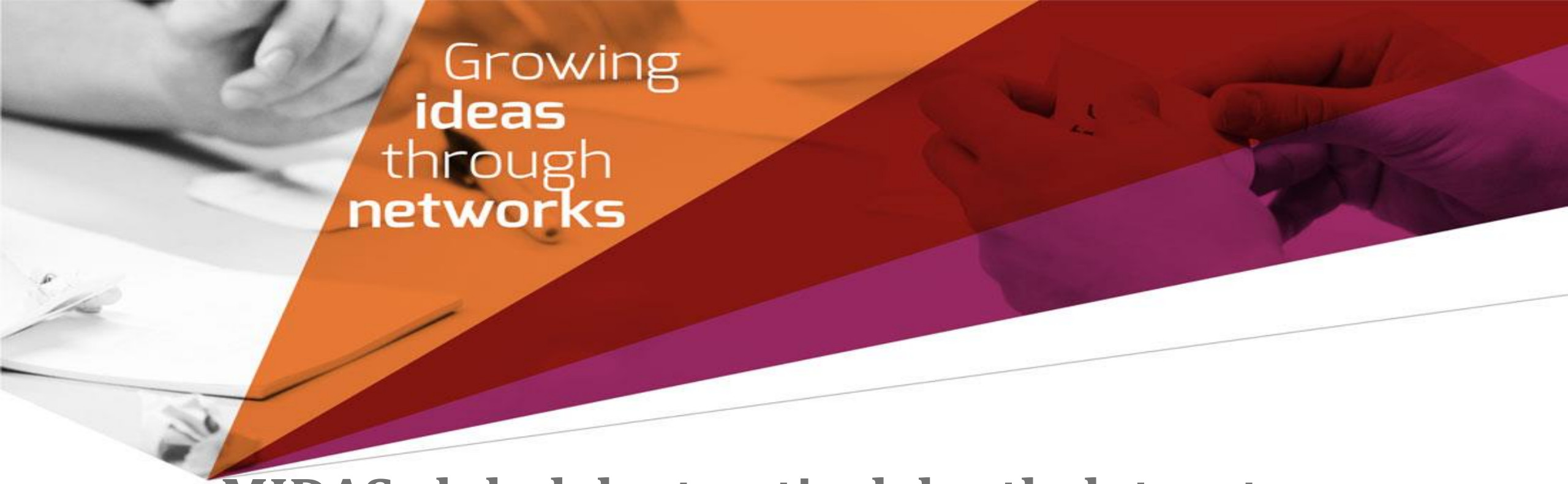
# Dust sources identification



# Recap and summary

- Development of the MIDAS global fine resolution dust optical depth dataset
- Feasibility of the MIDAS DOD product exploitation in various applications
- Description of dust aerosols' regime at global and regional scales
- Investigation of dust loads' temporal variation throughout the period 2003-2017
- Dust induced perturbations of the SW radiation reaching at the ground
- MIDAS data assimilation in the MONARCH model
- Identification of dust sources

cost
EUROPEAN COOPERATION IN SCIENCE & TECHNOLOGY




# MIDAS global dust optical depth dataset: Development and applications

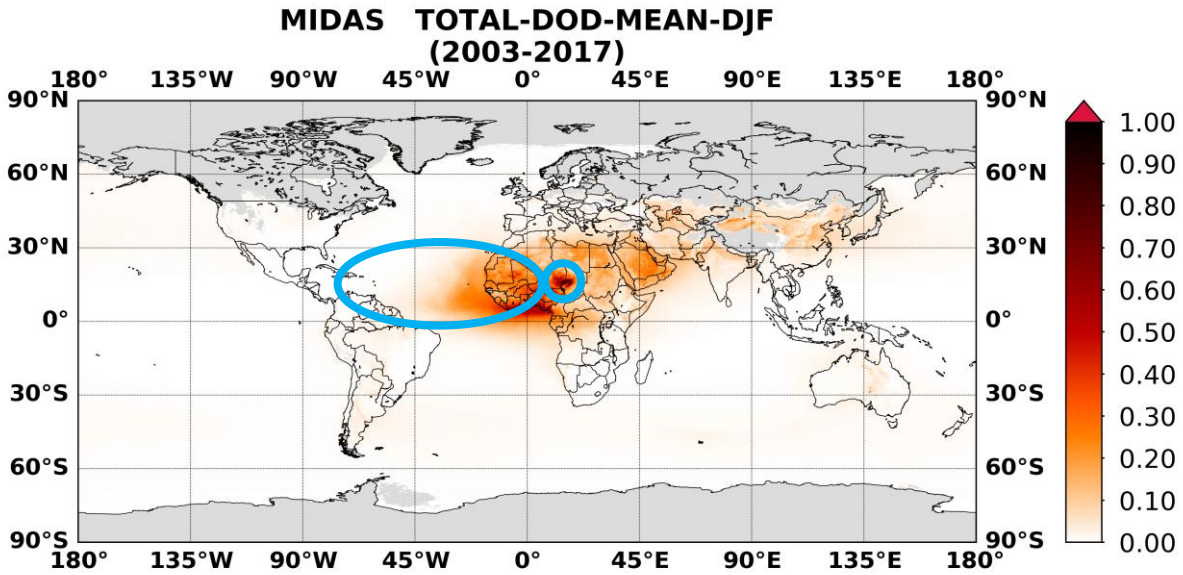
**Antonis Gkikas**

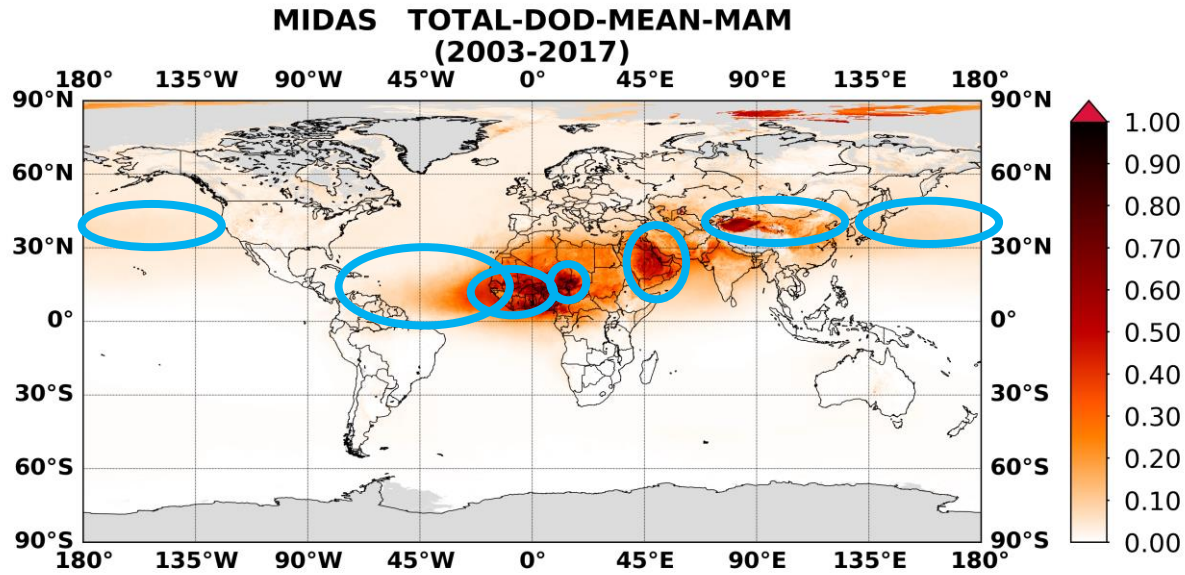
National Observatory of Athens (NOA)

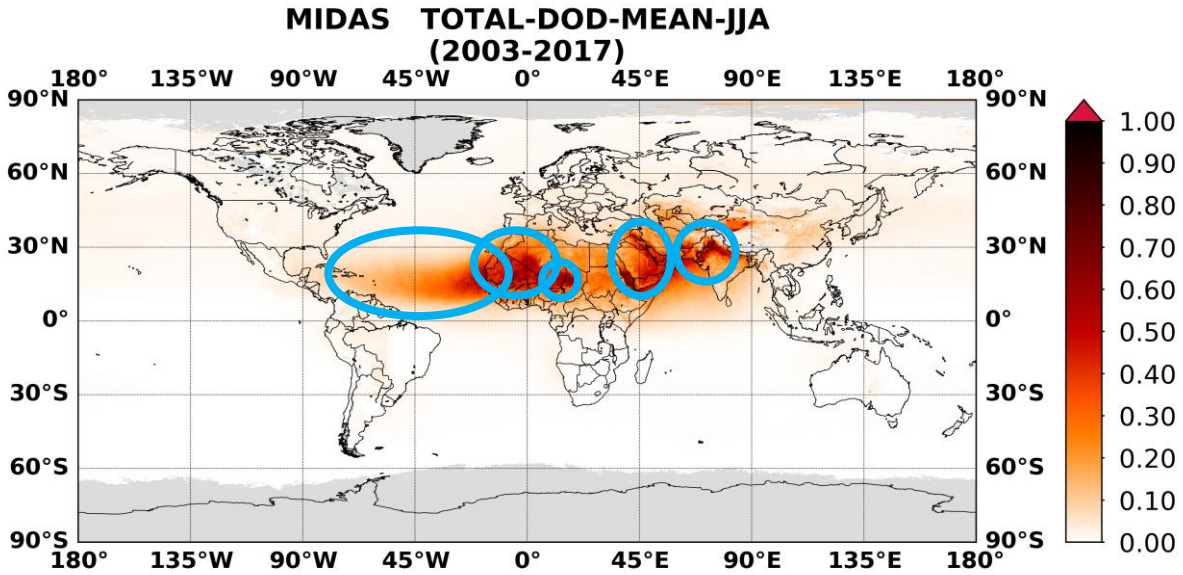
cost
EUROPEAN COOPERATION
IN SCIENCE & TECHNOLOGY

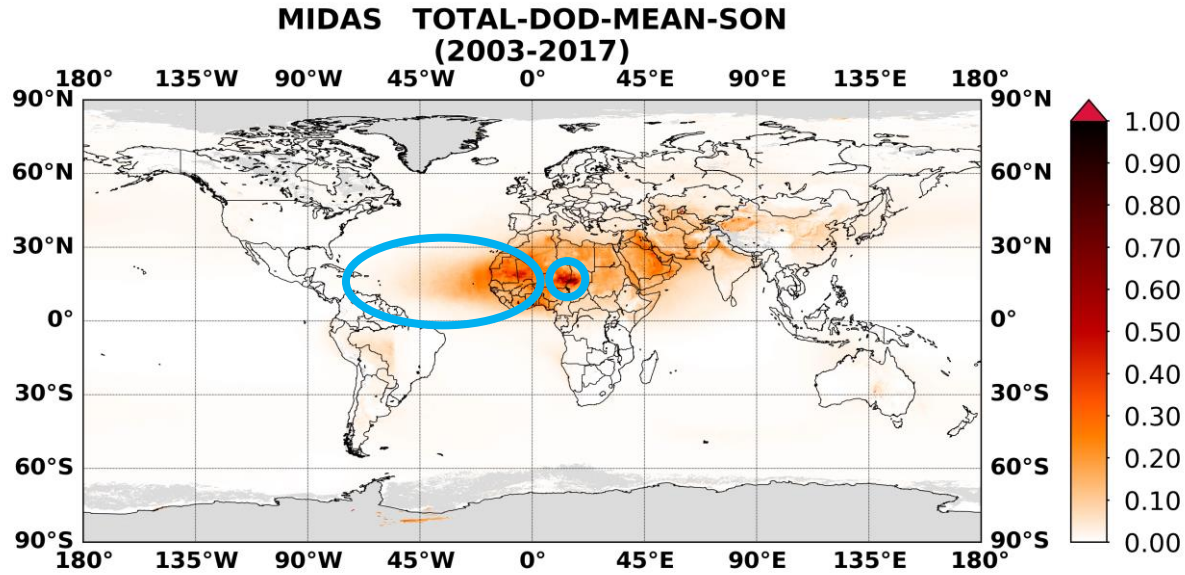
Funded by the Horizon 2020 Framework Programme
of the European Union

# MIDAS DOD seasonal global patterns

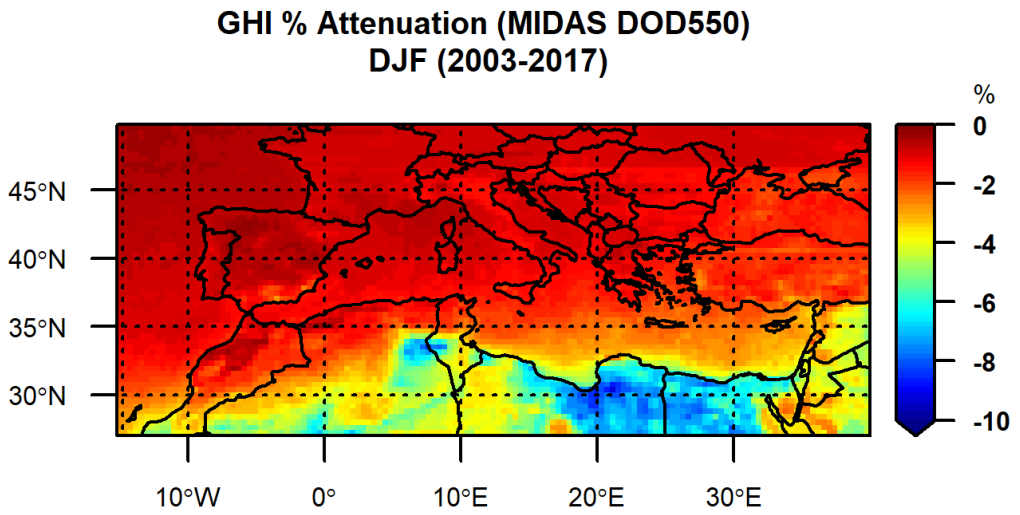


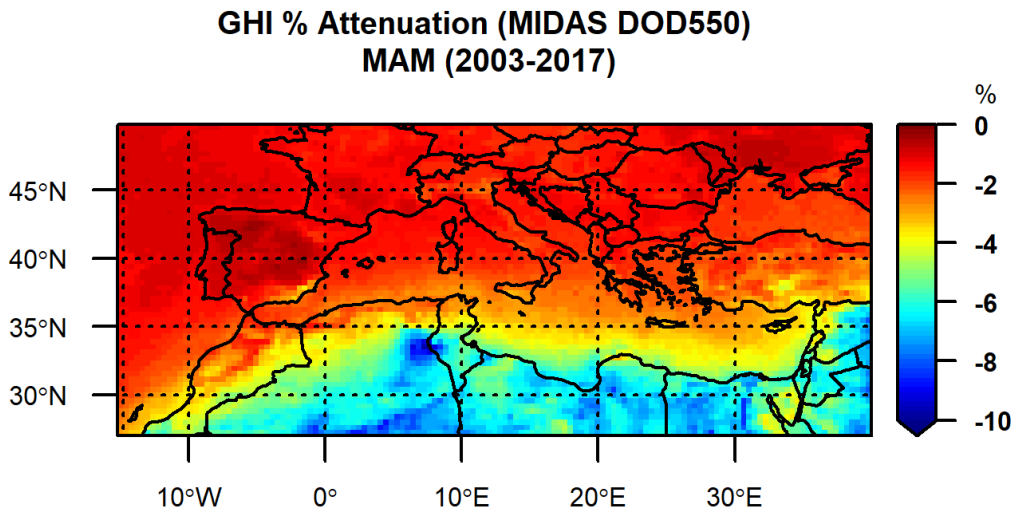



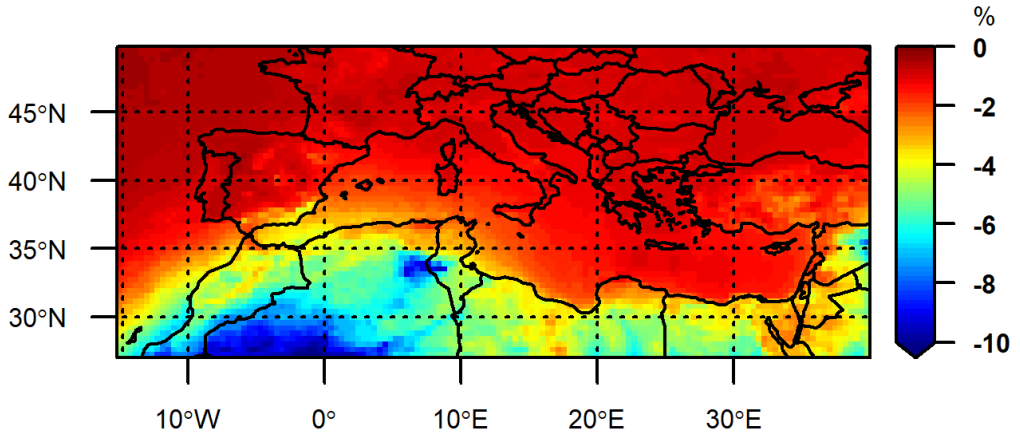



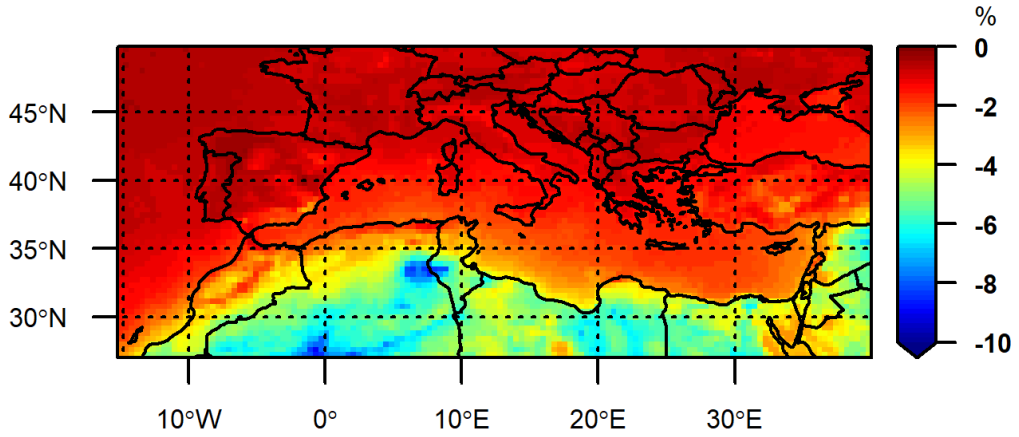
# Seasonal variability of the surface SW DREs




$$\frac{F_{dust} - F_{no-dust}}{F_{no-dust}} * 100\%$$




**Papachristopoulou et al. (in preparation)**